

Two-Stage Stochastic Optimization via Primal-Dual Decomposition and Deep Unrolling

An Liu, *Senior Member, IEEE*, Rui Yang, Tony Q. S. Quek, *Fellow, IEEE* and Min-Jian Zhao, *Member, IEEE*

Abstract—We consider a two-stage stochastic optimization problem, in which a long-term optimization variable is coupled with a set of short-term optimization variables in both objective and constraint functions. Despite that two-stage stochastic optimization plays a critical role in various engineering and scientific applications, there still lack efficient algorithms, especially when the long-term and short-term variables are coupled in the constraints. To overcome the challenge caused by tightly coupled stochastic constraints, we first establish a two-stage primal-dual decomposition (PDD) method to decompose the two-stage problem into a long-term problem and a family of short-term subproblems. Then we propose a PDD-based stochastic successive convex approximation (PDD-SSCA) algorithmic framework to find KKT solutions for two-stage stochastic optimization problems. At each iteration, PDD-SSCA first runs a short-term sub-algorithm to find stationary points of the short-term subproblems associated with a mini-batch of the state samples. Then it constructs a convex surrogate for the long-term problem based on the deep unrolling of the short-term sub-algorithm and the back propagation method. Finally, the optimal solution of the convex surrogate problem is solved to generate the next iterate. We establish the almost sure convergence of PDD-SSCA and customize the algorithmic framework to solve two important application problems. Simulations show that PDD-SSCA can achieve superior performance over existing solutions.

Index Terms—Two-stage stochastic optimization, primal-dual decomposition, Deep unrolling

I. INTRODUCTION

In this paper, we consider the following two-stage stochastic optimization problem:

$$\mathcal{P} : \min_{\mathbf{x}, \Theta} f_0(\mathbf{x}, \Theta) \triangleq \mathbb{E} [g_0(\mathbf{x}, \mathbf{y}(\boldsymbol{\xi}), \boldsymbol{\xi})], \quad (1)$$

$$\begin{aligned} \text{s.t. } f_i(\mathbf{x}, \Theta) \triangleq \mathbb{E} [g_i(\mathbf{x}, \mathbf{y}(\boldsymbol{\xi}), \boldsymbol{\xi})] &\leq 0, \quad i = 1, \dots, m \\ h_j(\mathbf{y}(\boldsymbol{\xi}), \boldsymbol{\xi}) &\leq 0, \quad j = 1, \dots, n, \quad \forall \boldsymbol{\xi} \in \Omega, \end{aligned} \quad (2)$$

where $\mathbf{x} \in \mathcal{X}$ is the *long-term (first stage) optimization variable*, with \mathcal{X} being the domain of \mathbf{x} ; $\boldsymbol{\xi}$ is a random state defined on the probability space $(\Omega, \mathcal{F}, \mathbb{P})$, with Ω being the sample space, \mathcal{F} being the σ -algebra generated by subsets of

This work was supported in part by the National Science Foundation of China under Grant 62071416, in part by the National Research Foundation, Singapore and Infocomm Media Development Authority under its Future Communications Research & Development Programme, in part by the SUTD Growth Plan Grant for AI, and in part by the SUTD-ZJU Seed Grant SUTD-ZJU (SD) 201909. Any opinions, findings and conclusions or recommendations expressed in this material are those of the author(s) and do not reflect the views of National Research Foundation, Singapore and Infocomm Media Development Authority. (Corresponding authors: An Liu; Min-Jian Zhao.)

An Liu, Rui Yang and Min-Jian Zhao are with the College of Information Science and Electronic Engineering, Zhejiang University, Hangzhou 310027, China (email: anliu@zju.edu.cn).

Tony Q. S. Quek is with the Information Systems Technology and Design Pillar, Singapore University of Technology and Design (email: tonyquek@sutd.edu.sg).

Ω , and \mathbb{P} being a probability measure defined on \mathcal{F} ; $\mathbf{y}(\boldsymbol{\xi})$ is the *short-term (second stage) optimization variable* under state $\boldsymbol{\xi}$; and $\Theta \triangleq \{\mathbf{y}(\boldsymbol{\xi}) \in \mathcal{Y}, \forall \boldsymbol{\xi}\}$ is the collection of the short-term optimization variables for all possible states, with \mathcal{Y} being the domain of the short-term optimization variable \mathbf{y} . $f_i(\mathbf{x}, \Theta) \leq 0, i = 1, \dots, m$ are called the long-term constraints and $h_j(\mathbf{y}(\boldsymbol{\xi}), \boldsymbol{\xi}) \leq 0, j = 1, \dots, n$ are called the short-term constraints under the state $\boldsymbol{\xi}$. Clearly, in \mathcal{P} , the long-term variable \mathbf{x} is adaptive to the distribution/statistics of the random state $\boldsymbol{\xi}$, while the short-term variable \mathbf{y} is adaptive to the realization of the random state $\boldsymbol{\xi}$.

The study of the stochastic optimization in Problem \mathcal{P} is motivated by the following observations. Many physical systems are not deterministic and we must take into account of the underlying random state $\boldsymbol{\xi}$ in modelling optimization problems. Moreover, in practice, some optimization variables have to be optimized before observing the realization of the state $\boldsymbol{\xi}$, while the other optimization variables can be optimized after observing the realization of the state $\boldsymbol{\xi}$. These two types of optimization variables can be modeled by the long-term optimization variable and short-term optimization variable, respectively. For example, consider a multi-access channel with K users. There are M antennas at the receiver and a single antenna at each user (transmitter). The receiver applies linear beamforming to decode the information, and the average data rate of user k is given by $\mathbb{E} \left[\log \left(1 + \frac{p_k |\mathbf{u}_k^H(\mathbf{a}) \mathbf{a}_k|}{1 + \sum_{l \neq k} p_l |\mathbf{u}_k^H(\mathbf{a}) \mathbf{a}_l|} \right) \right]$, where \mathbf{a}_k is the channel of user k , $\mathbf{a} = \{\mathbf{a}_k, \forall k\}$ is the aggregate channel state, p_k is the transmit power for user k , and $\mathbf{u}_k(\mathbf{a})$ is the receive beamforming vector of user k for given channel state \mathbf{a} . Suppose the users only know the channel statistics and the receiver has perfect channel state information (CSI) \mathbf{a} . As such, the transmit power p_k is a long-term optimization variable only adaptive to the channel statistics, and the receive beamforming vectors $\mathbf{u}_k^H(\mathbf{a}), \forall \mathbf{a}$ are short optimization variables adaptive to the CSI \mathbf{a} . The design goal is to minimize the total transmit power subject to the average data rate constraints for each user:

$$\begin{aligned} \min_{\{p_k, \mathbf{u}_k(\mathbf{a})\}} \sum_{k=1}^K p_k \quad (3) \\ \text{s.t. } \mathbb{E} \left[\log \left(1 + \frac{p_k |\mathbf{u}_k^H(\mathbf{a}) \mathbf{a}_k|}{1 + \sum_{l \neq k} p_l |\mathbf{u}_k^H(\mathbf{a}) \mathbf{a}_l|} \right) \right] \leq 0, \quad \forall k. \end{aligned}$$

Problem (3) is an instance of Problem \mathcal{P} with random state \mathbf{a} . In fact, many important engineering and scientific applications, such as those considered in wireless resource optimizations [1]–[3], transportation network design [4] and machine/deep learning [5]–[7], can be viewed as instances of the two-

stage stochastic optimization problem \mathcal{P} . Despite its wide applications, Problem \mathcal{P} is very challenging and there only exist solutions for some specific applications. The existing two-stage stochastic optimization algorithms can be classified into the following four classes.

Deterministic Algorithms based on Sample Average Approximation (SAA): In this class, problem \mathcal{P} is approximated as a deterministic optimization problem $\tilde{\mathcal{P}}$ by replacing the objective/constraint functions $f_i(\mathbf{x}, \Theta), i = 0, 1, \dots, m$ with their SAAs $\tilde{f}_i(\mathbf{x}, \Theta) \triangleq \frac{1}{T} \sum_{j=1}^T g_i(\mathbf{x}, \mathbf{y}(\boldsymbol{\xi}_j), \boldsymbol{\xi}_j), i = 0, 1, \dots, m$ using $T \gg 1$ state samples $\boldsymbol{\xi}_j, j = 1, \dots, T$. Then, various deterministic optimization algorithms such as majorization-minimization (MM) [8] and successive convex approximation (SCA) [9] can be used to solve the resulting deterministic optimization problem $\tilde{\mathcal{P}}$ to obtain an approximate solution for Problem \mathcal{P} . In order to achieve a good approximation, T is usually chosen to be a large number and thus the SAA-based deterministic algorithms suffer from very high complexity.

Primal-Dual Decomposition Algorithms: The primal-dual methods refer to the approaches which concurrently solving a primal problem (corresponding to the original optimization task) as well as a dual formulation of this problem [10]. Primal-dual methods have been primarily employed in convex optimization problems and they are usually not guaranteed to converge in the non-convex case [10]. In [11], a nonconvex primal-dual decomposition method is proposed for *separable optimization problem*, where the optimization variables are separable in both objective and constraint functions. However, it cannot be applied to our problem because: 1) the long-term and short-term optimization variables in \mathcal{P} are coupled together in the objective/constraint functions, which does not satisfy the separable assumption in [11]; 2) the nonconvex primal-dual decomposition method in [10] is only locally convergent to an (locally) optimal solution when the initial point is sufficiently close to it. In [12], a new primal-dual decomposition algorithm is proposed for two-stage stochastic optimization with a convex objective and stochastic recourse matrices. However, it does not work for non-convex stochastic optimization.

Two-stage Stochastic Algorithms with Increasing Batch Size: In this class, it is usually assumed that one independent state sample can be observed at the beginning of each iteration of the algorithm. Then, at the t -th iteration, the algorithm uses all the available t state samples observed in the previous t iterations to update the long-term variable and t short-term variables associated with the t state samples, whose complexity may become unacceptable when the number of iterations t becomes large. A famous example of this class is the stochastic cutting plane algorithm (SCPA), which only works for two-stage stochastic convex problems [1], [13]. In [3], an approximate stochastic cutting plane algorithm (AS-CPA) is proposed to find a sub-optimal solution for a class of two-stage stochastic non-convex optimization problems with piece-wise linear objective functions. In [2], an alternating optimization (AO) algorithm with increasing batch size is proposed to find a stationary point for a two-stage stochastic non-convex optimization problem.

Two-stage Stochastic Algorithm with Finite Batch Size:

For the special case when the long-term and short-term variables are decoupled in the constraint, i.e., when $m = 0$ and the coupled constraints $f_i(\mathbf{x}, \Theta) \leq 0$ is absent, a two-stage stochastic algorithm called TOSCA with finite batch size is proposed in [14] to find a stationary point of Problem \mathcal{P} . In this case, it is assumed that a finite batch of $B \geq 1$ independent state samples can be observed at the beginning of each iteration. Then, at each iteration, the TOSCA algorithm uses B state samples to update the long-term variable and B short-term variables associated with the B state samples. The batch size B can be chosen to achieve a good tradeoff between the per-iteration complexity and the convergence speed.

Deep Learning (DL) Algorithms: Recently, DL has been widely applied to solve complicated optimization problems in various application areas [15]–[17]. For example, [15] is one of the pioneer works to consider resource allocation using DL-based optimization technique. In [17], the implementability of the global optimal solution with DL is demonstrated for a non-convex power allocation problem. A few DL algorithms have also been proposed to solve \mathcal{P} for the special case when the long-term variable \mathbf{x} is absent and only the short-term variables $\mathbf{y}(\boldsymbol{\xi})$ is present [6], [7], [18]. In this case, we can use a DNN $\phi(\boldsymbol{\xi}; \boldsymbol{\theta})$ to approximate the optimal solution $\mathbf{y}^*(\boldsymbol{\xi})$ and the optimal parameter $\boldsymbol{\theta}^*$ for the DNN can be found by solving the following unsupervised DL problem:

$$\begin{aligned} \min_{\boldsymbol{\theta}} \mathbb{E} [g_0(\phi(\boldsymbol{\xi}; \boldsymbol{\theta}), \boldsymbol{\xi})], \\ \text{s.t. } \mathbb{E} [g_i(\phi(\boldsymbol{\xi}; \boldsymbol{\theta}), \boldsymbol{\xi})] \leq 0, i = 1, \dots, m \\ h_j(\phi(\boldsymbol{\xi}; \boldsymbol{\theta}), \boldsymbol{\xi}) \leq 0, j = 1, \dots, n, \forall \boldsymbol{\xi}. \end{aligned} \quad (4)$$

However, existing DL optimizers are not suitable for handling complicated stochastic constraints in (4) [18]. To resolve this issue, a penalizing method is applied to transform the original constrained training problem to an unconstrained one by augmenting a penalty term associated with the complicated constraints into the objective function [6], [7]. In [18], a primal-dual method is employed to solve the constrained training problem in (4). However, when both the objective and constraint functions in (4) are non-convex, the methods in [6], [7], [18] cannot guarantee the convergence to a feasible stationary point of the original problem \mathcal{P} . Moreover, the DNN solution $\phi(\boldsymbol{\xi}; \boldsymbol{\theta})$ does not exploit the specific problem structure and the number of parameters $\boldsymbol{\theta}$ is usually large, leading to a high complexity and slow convergence of the DL algorithms.

In summary, there still lacks efficient algorithms for the two-stage stochastic optimization problem \mathcal{P} , especially when the long-term and short-term variables are tightly coupled in the constraints. In this paper, we propose a two-stage stochastic optimization algorithmic framework based on a primal-dual decomposition method and deep unrolling, to overcome the disadvantages of the above existing algorithms. The main contributions are summarized as follows.

- **Two-stage primal-dual decomposition method:** The existing primal-dual (decomposition) methods cannot handle the tightly coupled non-convex stochastic constraints containing both the long-term and short-term variables, as

explained above. To overcome this challenge, we establish a novel two-stage primal-dual decomposition method to decompose \mathcal{P} into a family of short-term subproblems $\mathcal{P}_S(\mathbf{x}, \boldsymbol{\lambda}, \boldsymbol{\xi})$, $\forall \boldsymbol{\xi}$ for fixed long-term variable \mathbf{x} and Lagrange multipliers $\boldsymbol{\lambda}$, and a long-term problem \mathcal{P}_L with both \mathbf{x} and $\boldsymbol{\lambda}$ as the optimization variables, where $\boldsymbol{\lambda} = [\lambda_1, \dots, \lambda_m]^T \succeq \mathbf{0}$ are the Lagrange multipliers associated with the long-term constraints $f_i(\mathbf{x}, \boldsymbol{\lambda}) \leq 0$, $i = 1, \dots, m$. Since this method involves solving both a primal problem and a “mixed-primal-dual” problem (i.e., a problem containing both primal variable \mathbf{x} and dual variable $\boldsymbol{\lambda}$), and the primal problem is further decomposed into short-term subproblems, we call it the two-stage “primal-dual decomposition” method. Such a decomposition method is clearly different from the existing primal-dual methods in [10]–[12]. We establish the global and local optimality of this decomposition method in Theorem 1 and 2, respectively, whose proofs are non-trivial as shown in Appendix 1 and 2.

- **A two-stage stochastic optimization framework:** We propose a primal-dual decomposition based stochastic successive convex approximation (PDD-SSCA) framework which can be applied to a class of two-stage stochastic optimization problems that satisfy certain smooth conditions as will be given in Assumption 1, without any other restrictive assumptions. For example, the long-term and short-term variables can have tight coupling in the constraints and all objective and constraint functions can be non-convex. As such, this optimization framework opens the door to solving two-stage stochastic optimization problems that occur in many new applications. We establish the convergence of PDD-SSCA to KKT solutions of \mathcal{P} under mild conditions. To the best of our knowledge, the proposed PDD-CSSCA is the first algorithm that can guarantee the convergence to a KKT solution of a two-stage stochastic optimization problem with tightly coupled non-convex stochastic constraints.
- **Specific PDD-SSCA algorithm design for some important applications:** We apply PDD-SSCA to solve two important problems in wireless resource allocation and hybrid analog-digital signal processing, respectively. We believe that the proposed PDD-SSCA solutions for these problems alone are of great interest to the community.

The rest of the paper is organized as follows. The assumptions on the problem formulation is given in Section II, together with some application examples. The primal-dual decomposition method for two-stage stochastic optimization is established in Section III. The PDD-SSCA algorithm and the convergence analysis are presented in Section IV, and some implementation details are discussed in Section V. Section VI applies PDD-SSCA to solve two important application problems. Finally, the conclusion is given in Section VI-C.

II. PROBLEM FORMULATION

A. Assumptions on Problem \mathcal{P}

We make the following assumptions on Problem \mathcal{P} .

Assumption 1 (Assumptions on Problem \mathcal{P}).

- 1) $\mathcal{X} \subseteq \mathbb{R}^{n_x}$ and $\mathcal{Y} \subseteq \mathbb{R}^{n_y}$ for some positive integers n_x and n_y . Moreover, \mathcal{X}, \mathcal{Y} are compact and convex.
- 2) The functions $g_i(\mathbf{x}, \mathbf{y}, \boldsymbol{\xi})$, $i = 0, \dots, m$ are real valued and continuously differentiable functions in $\mathbf{x} \in \mathcal{X}, \mathbf{y} \in \mathcal{Y}$.
- 3) The functions $h_j(\mathbf{y}, \boldsymbol{\xi})$, $j = 0, \dots, n$ are real valued and continuously differentiable functions in $\mathbf{y} \in \mathcal{Y}$.
- 4) For any $i \in \{0, \dots, m\}$ and $\boldsymbol{\xi} \in \Omega$, the function $g_i(\mathbf{x}, \mathbf{y}, \boldsymbol{\xi})$, its derivative w.r.t. \mathbf{x} and \mathbf{y} , and its second-order derivative w.r.t. \mathbf{x} and \mathbf{y} , are uniformly bounded.
- 5) For any $j \in \{1, \dots, n\}$ and $\boldsymbol{\xi} \in \Omega$, the function $h_j(\mathbf{y}, \boldsymbol{\xi})$, its derivative w.r.t. \mathbf{y} , and its second-order derivative w.r.t. \mathbf{y} , are uniformly bounded.
- 6) For any $\boldsymbol{\xi} \in \Omega$, the short-term constraints are feasible, i.e., $\exists \mathbf{y} \in \mathcal{Y}$, such that $h_j(\mathbf{y}, \boldsymbol{\xi}) \leq 0, \forall j$. Moreover, Problem \mathcal{P} is feasible.

These conditions are standard and are satisfied for a large class of problems. For ease of exposition, we assume \mathbf{x}, \mathbf{y} are real vectors. Nevertheless, the proposed algorithm can be directly applied to the case with complex optimization variables \mathbf{x}, \mathbf{y} , by treating each function $g_i(\mathbf{x}, \mathbf{y}, \boldsymbol{\xi})$ in the problem as a real valued function of real vectors $[\text{Re}[\mathbf{x}]; \text{Im}[\mathbf{x}]]$ and $[\text{Re}[\mathbf{y}]; \text{Im}[\mathbf{y}]]$.

B. Examples of Problem \mathcal{P}

Problem \mathcal{P} embraces many applications. In the following, we give two important examples.

Example 1 (Cognitive Multiple Access Channels [19]). Consider a multi-user uplink cognitive (CR) network [19] with one licensed primary user (PU) and N secondary users (SUs). The SUs share time and frequency resources with the PU and desire to transmit their data to a secondary base station (SBS). The SBS and all users are all equipped with only a single antenna. Let a_i and b_i denote the channel gain from SU i to the SBS and the PU, respectively. The average sum capacity maximization problem can be formulated as [19]

$$\begin{aligned} \max_{\{p(\mathbf{a}, \mathbf{b})\}} \mathbb{E} \left[\log \left(1 + \sum_{i=1}^N a_i p_i(\mathbf{a}, \mathbf{b}) \right) \right], \quad (5) \\ \text{s.t. } \mathbb{E} [p_i(\mathbf{a}, \mathbf{b})] \leq P_i, \quad i = 1, \dots, N \\ \mathbb{E} \left[\sum_{i=1}^N b_i p_i(\mathbf{a}, \mathbf{b}) \right] \leq \Gamma, \\ p_i(\mathbf{a}, \mathbf{b}) \geq 0, \quad i = 1, \dots, N, \forall \mathbf{a}, \mathbf{b}, \end{aligned}$$

where $\mathbf{a} = [a_1, \dots, a_N]^T$, $\mathbf{b} = [b_1, \dots, b_N]^T$, $p_i(\mathbf{a}, \mathbf{b})$ is the transmit power at SU i when the channel state is \mathbf{a}, \mathbf{b} , $\mathbf{p}(\mathbf{a}, \mathbf{b}) = [p_1(\mathbf{a}, \mathbf{b}), \dots, p_N(\mathbf{a}, \mathbf{b})]^T$, P_i and Γ stand for the long-term transmit power budget at SU i and the interference threshold constraint for the PU, respectively. Clearly, problem (5) is a special case of \mathcal{P} with short-term variables $\mathbf{p}(\mathbf{a}, \mathbf{b})$, $\forall \mathbf{a}, \mathbf{b}$ only. The random state is the channel state \mathbf{a}, \mathbf{b} .

Example 2 (Power Minimization for Two-timescale hybrid beamforming [20]). Massive MIMO is considered as one of

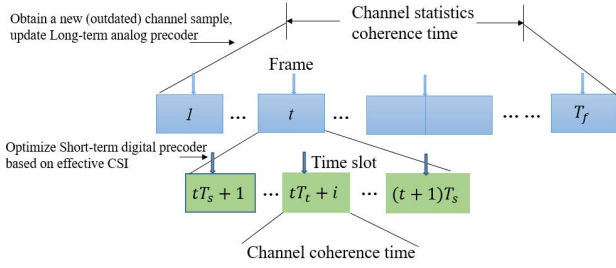


Figure 1: Timeline (frame structure) of two-timescale hybrid beamforming

the key technologies in 5G wireless systems. Consider a multi-user massive MIMO downlink system where a base station (BS) serves K single-antenna users. The BS is equipped with $M \gg 1$ antennas and S transmit RF chains, where $K \leq S < M$. Two-timescale hybrid beamforming is employed at the BS to support simultaneous transmissions to the K users, with reduced hardware cost and channel state information (CSI) signaling overhead [20]–[22]. Specifically, the precoder is split into a baseband precoder and an RF precoder as $\mathbf{F}\mathbf{G}$, where $\mathbf{G} = [\mathbf{g}_1, \dots, \mathbf{g}_K] \in \mathbb{C}^{S \times K}$ is the baseband precoder, and $\mathbf{F} \in \mathbb{C}^{M \times S}$ is the RF precoder using the RF phase shifting network [23]. Hence, all elements of \mathbf{F} have equal magnitude, i.e., $F_{m,s} = e^{j\theta_{m,s}}$, where $\theta_{m,s}$ is the phase of the (m, s) -th element $F_{m,s}$ of \mathbf{F} . The RF precoder \mathbf{F} can be represented by a phase vector $\boldsymbol{\theta} \in \mathbb{R}^{MS}$ whose $((j-1)M + i)$ -th element is $\theta_{i,j}$.

We focus on a coherence time interval of channel statistics within which the channel statistics (distribution) are assumed to be constant. The coherence time of channel statistics is divided into T_f frames and each frame consists of T_s time slots, as illustrated in Fig. 1. The channel state $\mathbf{H} = [\mathbf{h}_1, \dots, \mathbf{h}_K]^H \in \mathbb{C}^{K \times M}$ is assumed to be constant within each time slot, where $\mathbf{h}_k \in \mathbb{C}^M$ is the channel vector of user k . We assume that the BS can obtain the real-time effective CSI $\widetilde{\mathbf{H}} = \mathbf{H}\mathbf{F} \in \mathbb{C}^{K \times S}$ at each time slot, and one outdated channel sample \mathbf{H} at each frame. In the THP design, the analog precoder \mathbf{F} is only updated once per frame based on the outdated channel sample \mathbf{H} to achieve massive MIMO array gain. The digital precoder \mathbf{G} is adaptive to the real-time effective CSI $\widetilde{\mathbf{H}} \in \mathbb{C}^{K \times S}$ to achieve the spatial multiplexing gain. Note that the effective CSI $\widetilde{\mathbf{H}}$ usually has much lower dimension than the full channel sample \mathbf{H} . Therefore, it is possible to obtain the real-time effective CSI $\widetilde{\mathbf{H}}$ at each time slot by sending pilot signals with analog precoder \mathbf{F} . However, we can only obtain one outdated full channel sample \mathbf{H} at each frame because obtaining the real-time full CSI \mathbf{H} per time slot will cause unacceptable CSI signaling overhead in massive MIMO. Therefore, we cannot optimize both the analog and digital precoders based on the real-time full CSI \mathbf{H} at each time slot. \mathbf{F} and \mathbf{G} have to be optimized at different timescale based on the outdated channel sample \mathbf{H} and real-time effective CSI $\widetilde{\mathbf{H}}$, respectively, using e.g., the proposed PDD-SSCA algorithm. In this example, each frame corresponds to an iteration of PDD-SSCA.

For given RF precoding phase vector $\boldsymbol{\theta}$, baseband precoder \mathbf{G} and channel realization \mathbf{H} , the data rate of user k is given by

$$r_k(\boldsymbol{\theta}, \mathbf{G}, \mathbf{H}) = \log \left(1 + \frac{|\mathbf{h}_k^H \mathbf{F} \mathbf{g}_k|^2}{\sum_{i \neq k} |\mathbf{h}_k^H \mathbf{F} \mathbf{g}_i|^2 + 1} \right). \quad (6)$$

Note that \mathbf{F} is a function of $\boldsymbol{\theta}$. Consider the problem of average transmit power minimization for the above massive MIMO system with individual average rate constraint for each user, which can be formulated as:

$$\begin{aligned} \min_{\boldsymbol{\theta}, \{\mathbf{G}(\mathbf{H}), \forall \mathbf{H}\}} \mathbb{E} \left[\text{Tr} \left(\mathbf{F} \mathbf{G}(\mathbf{H}) \mathbf{G}^H(\mathbf{H}) \mathbf{F}^H \right) \right], \quad (7) \\ \text{s.t. } \mathbb{E} [r_k(\boldsymbol{\theta}, \mathbf{G}(\mathbf{H}), \mathbf{H})] \geq \gamma_k, k = 1, \dots, K, \end{aligned}$$

where γ_k is the throughput requirement for user k . Problem (7) is an instance of Problem \mathcal{P} with random state \mathbf{H} .

C. KKT Solution of Problem \mathcal{P}

Since Problem \mathcal{P} is in general non-convex, we focus on designing an efficient algorithm to find KKT solutions of Problem \mathcal{P} , defined as follows.

Definition 1 (KKT solution of \mathcal{P}). A solution $(\mathbf{x}^* \in \mathcal{X}, \Theta^* = \{\mathbf{y}^*(\boldsymbol{\xi}) \in \mathcal{Y}, \forall \boldsymbol{\xi}\})$ is called a KKT solution of Problem \mathcal{P} , if there exist long-term Lagrange multipliers $\boldsymbol{\lambda} = [\lambda_1, \dots, \lambda_m]^T \succeq \mathbf{0}$ associated with the long-term constraints and short-term Lagrange multipliers $\nu_j(\boldsymbol{\xi}) \geq 0, \forall j, \forall \boldsymbol{\xi}$ associated with the short-term constraints, such that the following conditions are satisfied:

- 1) For every $\boldsymbol{\xi} \in \Omega$ outside a set of probability zero, we have

$$\begin{aligned} \partial_{\mathbf{y}} g_0(\mathbf{x}^*, \mathbf{y}^*(\boldsymbol{\xi}), \boldsymbol{\xi}) \\ + \sum_i \lambda_i \partial_{\mathbf{y}} g_i(\mathbf{x}^*, \mathbf{y}^*(\boldsymbol{\xi}), \boldsymbol{\xi}) \\ + \sum_j \nu_j(\boldsymbol{\xi}) \partial_{\mathbf{y}} h_j(\mathbf{y}^*(\boldsymbol{\xi}), \boldsymbol{\xi}) = \mathbf{0}, \\ h_j(\mathbf{y}^*(\boldsymbol{\xi}), \boldsymbol{\xi}) \leq 0, j = 1, \dots, n, \\ \nu_j(\boldsymbol{\xi}) h_j(\mathbf{y}^*(\boldsymbol{\xi}), \boldsymbol{\xi}) = 0, j = 1, \dots, n. \quad (8) \end{aligned}$$

where $\partial_{\mathbf{y}} g_i(\mathbf{x}^*, \mathbf{y}^*(\boldsymbol{\xi}), \boldsymbol{\xi})$ and $\partial_{\mathbf{y}} h_j(\mathbf{y}^*(\boldsymbol{\xi}), \boldsymbol{\xi})$ are the partial derivatives of $g_i(\mathbf{x}^*, \mathbf{y}, \boldsymbol{\xi})$ and $h_j(\mathbf{y}, \boldsymbol{\xi})$ w.r.t. \mathbf{y} at $\mathbf{y} = \mathbf{y}^*(\boldsymbol{\xi})$, respectively.

- 2)

$$\begin{aligned} \partial_{\mathbf{x}} f_0(\mathbf{x}^*, \Theta^*) + \sum_i \lambda_i \partial_{\mathbf{x}} f_i(\mathbf{x}^*, \Theta^*) = \mathbf{0}, \\ f_i(\mathbf{x}^*, \Theta^*) \leq 0, \forall i \quad (9) \end{aligned}$$

where $\partial_{\mathbf{x}} f_i(\mathbf{x}^*, \Theta^*)$ is the partial derivative of $f_i(\mathbf{x}, \Theta^*)$ w.r.t. \mathbf{x} at $\mathbf{x} = \mathbf{x}^*$.

- 3)

$$\lambda_i f_i(\mathbf{x}^*, \Theta^*) = 0, i = 1, \dots, m. \quad (10)$$

III. TWO-STAGE PRIMAL-DUAL DECOMPOSITION METHOD

A. Two-Stage Primal-Dual Decomposition for \mathcal{P}

One major challenge of solving \mathcal{P} is that, the long-term variable \mathbf{x} and the short-term variables $\mathbf{y}(\boldsymbol{\xi})$'s for different states are coupled together in a complicated manner via the long-term constraint. As discussed in the introduction, the existing primal-dual (decomposition) methods in [10]–[12] cannot work for problem \mathcal{P} with tightly coupled non-convex stochastic constraints. To overcome this challenge, we prove a novel primal-dual decomposition method to decouple the optimization variables. Specifically, for a fixed long-term variable \mathbf{x} and long-term Lagrange multipliers $\boldsymbol{\lambda}$, let $\phi_{\mathbf{x},\boldsymbol{\lambda}}^*$ denote the *optimal short-term policy*, which is defined a mapping from Ω to \mathcal{Y} such that $\mathbf{y}^*(\mathbf{x}, \boldsymbol{\lambda}, \boldsymbol{\xi}) = \phi_{\mathbf{x},\boldsymbol{\lambda}}^*(\boldsymbol{\xi})$ is the optimal solution of the following *short-term subproblem*:

$$\begin{aligned} \mathcal{P}_S(\mathbf{x}, \boldsymbol{\lambda}, \boldsymbol{\xi}) : \min_{\mathbf{y}} g_0(\mathbf{x}, \mathbf{y}, \boldsymbol{\xi}) + \sum_i \lambda_i g_i(\mathbf{x}, \mathbf{y}, \boldsymbol{\xi}), \quad (11) \\ \text{s.t. } h_j(\mathbf{y}, \boldsymbol{\xi}) \leq 0, \quad j = 1, \dots, n. \end{aligned}$$

Note that the optimal short-term policy is not necessarily unique and the set of all optimal short-term policies is denoted as $\Phi_{\mathbf{x},\boldsymbol{\lambda}}^*$. When $\Phi_{\mathbf{x},\boldsymbol{\lambda}}^*$ have multiple elements, we choose one optimal short-term policy $\phi_{\mathbf{x},\boldsymbol{\lambda}}^*$ as $\phi_{\mathbf{x},\boldsymbol{\lambda}}^* \in \operatorname{argmin}_{\phi \in \Phi_{\mathbf{x},\boldsymbol{\lambda}}^*} \max_{i \in \{1, \dots, m\}} \mathbb{E}[g_i(\mathbf{x}, \phi(\boldsymbol{\xi}), \boldsymbol{\xi})]$, where $\Phi_{\mathbf{x},\boldsymbol{\lambda}}^* \triangleq \operatorname{argmin}_{\phi \in \Phi_{\mathbf{x},\boldsymbol{\lambda}}^*} \sum_i \lambda_i \mathbb{E}[g_i(\mathbf{x}, \phi(\boldsymbol{\xi}), \boldsymbol{\xi})]$ is the set of all optimal short-term policies that minimize $\sum_i \lambda_i \mathbb{E}[g_i(\mathbf{x}, \phi(\boldsymbol{\xi}), \boldsymbol{\xi})]$. In other words, we choose $\phi_{\mathbf{x},\boldsymbol{\lambda}}^*$ as an optimal short-term policy which is most likely to satisfy the constraints and complementary slackness condition of the original Problem \mathcal{P} . With the optimal short-term policy $\phi_{\mathbf{x},\boldsymbol{\lambda}}^*$ and $\{\mathbf{y}^*(\mathbf{x}, \boldsymbol{\lambda}, \boldsymbol{\xi}) = \phi_{\mathbf{x},\boldsymbol{\lambda}}^*(\boldsymbol{\xi}), \forall \boldsymbol{\xi}\}$ chosen according to the above rule, we formulate the following long-term problem

$$\begin{aligned} \mathcal{P}_L : \min_{\mathbf{x}, \boldsymbol{\lambda}} f_0^*(\mathbf{x}, \boldsymbol{\lambda}) \triangleq \mathbb{E}[g_0(\mathbf{x}, \mathbf{y}^*(\mathbf{x}, \boldsymbol{\lambda}, \boldsymbol{\xi}), \boldsymbol{\xi})], \quad (12) \\ \text{s.t. } f_i^*(\mathbf{x}, \boldsymbol{\lambda}) \triangleq \mathbb{E}[g_i(\mathbf{x}, \mathbf{y}^*(\mathbf{x}, \boldsymbol{\lambda}, \boldsymbol{\xi}), \boldsymbol{\xi})] \leq 0, \quad \forall i. \end{aligned}$$

Problem \mathcal{P}_L only contains long-term variables $\mathbf{x}, \boldsymbol{\lambda}$. Now we are ready to establish a two-stage primal-dual decomposition theorem for Problem \mathcal{P} .

Theorem 1 (Two-stage Primal-Dual Decomposition). *Let $(\mathbf{x}^*, \boldsymbol{\lambda}^*)$ denote any optimal solution of \mathcal{P}_L . Define*

$$\begin{aligned} G_i^{\min}(\mathbf{x}) &\triangleq \min_{\Theta} f_i(\mathbf{x}, \Theta), \quad \text{s.t. (2) is satisfied,} \\ G_i^{\max}(\mathbf{x}) &\triangleq \max_{\Theta} f_i(\mathbf{x}, \Theta) \quad \text{s.t. (2) is satisfied.} \end{aligned}$$

If there exists an optimal solution of \mathcal{P} , denoted as $\mathbf{x}^\circ, \Theta^\circ = \{\mathbf{y}^\circ(\boldsymbol{\xi}), \forall \boldsymbol{\xi}\}$, such that there exist arbitrary small numbers $\delta_i \in (0, G_i^{\max}(\mathbf{x}^\circ) - G_i^{\min}(\mathbf{x}^\circ))$, $i = 1, \dots, m$, then $(\mathbf{x}^, \Theta^* = \{\mathbf{y}^*(\mathbf{x}^*, \boldsymbol{\lambda}^*, \boldsymbol{\xi}) \in \mathcal{Y}, \forall \boldsymbol{\xi}\})$ is also the optimal solution of \mathcal{P} .*

Please refer to Appendix 1 for the proof.

Note that the condition in Theorem 1 means that for fixed long-term variable \mathbf{x}° , the maximum value of the constraint function $G_i^{\max}(\mathbf{x}^\circ)$ is strictly larger than the minimum value

of the constraint function $G_i^{\min}(\mathbf{x}^\circ)$, which can be easily satisfied in practice. Theorem 1 essentially states that \mathcal{P} can be decomposed into a family of short-term subproblems $\mathcal{P}_S(\mathbf{x}, \boldsymbol{\lambda}, \boldsymbol{\xi})$ for fixed $\mathbf{x}, \boldsymbol{\lambda}, \boldsymbol{\xi}$ and a long-term problem \mathcal{P}_L with $\mathbf{x}, \boldsymbol{\lambda}$ as optimization variables. However, it is not convenient to directly apply Theorem 1 for algorithm design because such a decomposition requires the optimal solution of the short-term subproblem $\mathcal{P}_S(\mathbf{x}, \boldsymbol{\lambda}, \boldsymbol{\xi})$ for each $\boldsymbol{\xi}$, which is difficult to obtain in practice, especially when $\mathcal{P}_S(\mathbf{x}, \boldsymbol{\lambda}, \boldsymbol{\xi})$ is non-convex. Therefore, in the following, we will establish a relaxed primal-dual decomposition method which does not require the optimal solution of $\mathcal{P}_S(\mathbf{x}, \boldsymbol{\lambda}, \boldsymbol{\xi})$. Consequently, the relaxed primal-dual decomposition method can be applied to design an efficient algorithm to find KKT solutions of \mathcal{P} up to certain tolerable error.

B. Relaxed Two-Stage Primal-Dual Decomposition

Let $\mathbf{y}^J(\mathbf{x}, \boldsymbol{\lambda}, \boldsymbol{\xi})$ denote a stationary point (up to certain tolerable error) of the *short-term subproblem* $\mathcal{P}_S(\mathbf{x}, \boldsymbol{\lambda}, \boldsymbol{\xi})$ obtained by running a *short-term sub-algorithm* for J iterations. The short-term sub-algorithm is basically an iterative algorithm to find a stationary point of the short-term subproblem $\mathcal{P}_S(\mathbf{x}, \boldsymbol{\lambda}, \boldsymbol{\xi})$. In other words, $\mathbf{y}^J(\mathbf{x}, \boldsymbol{\lambda}, \boldsymbol{\xi})$ satisfies the KKT conditions of $\mathcal{P}_S(\mathbf{x}, \boldsymbol{\lambda}, \boldsymbol{\xi})$ (up to certain tolerable error) as

$$\begin{aligned} &\left\| \begin{aligned} &\partial_{\mathbf{y}} g_0(\mathbf{x}, \mathbf{y}^J(\mathbf{x}, \boldsymbol{\lambda}, \boldsymbol{\xi}), \boldsymbol{\xi}) \\ &+ \sum_i \lambda_i \partial_{\mathbf{y}} g_i(\mathbf{x}, \mathbf{y}^J(\mathbf{x}, \boldsymbol{\lambda}, \boldsymbol{\xi}), \boldsymbol{\xi}) \\ &+ \sum_j \nu_j(\mathbf{x}, \boldsymbol{\lambda}, \boldsymbol{\xi}) \partial_{\mathbf{y}} h_j(\mathbf{y}^J(\mathbf{x}, \boldsymbol{\lambda}, \boldsymbol{\xi}), \boldsymbol{\xi}) \end{aligned} \right\| = e_1^J(\mathbf{x}, \boldsymbol{\lambda}, \boldsymbol{\xi}), \\ &h_j(\mathbf{y}^J(\mathbf{x}, \boldsymbol{\lambda}, \boldsymbol{\xi}), \boldsymbol{\xi}) \leq e_2^J(\mathbf{x}, \boldsymbol{\lambda}, \boldsymbol{\xi}), \quad j = 1, \dots, n, \\ &\nu_j(\mathbf{x}, \boldsymbol{\lambda}, \boldsymbol{\xi}) h_j(\mathbf{y}^J(\mathbf{x}, \boldsymbol{\lambda}, \boldsymbol{\xi}), \boldsymbol{\xi}) = e_{3,j}^J(\mathbf{x}, \boldsymbol{\lambda}, \boldsymbol{\xi}), \quad j = 1, \dots, n, \end{aligned} \quad (13)$$

where $\nu_j(\mathbf{x}, \boldsymbol{\lambda}, \boldsymbol{\xi}) \geq 0, \forall j$ are the short-term Lagrange multipliers, and $e_1^J(\mathbf{x}, \boldsymbol{\lambda}, \boldsymbol{\xi}), e_2^J(\mathbf{x}, \boldsymbol{\lambda}, \boldsymbol{\xi}), e_{3,j}^J(\mathbf{x}, \boldsymbol{\lambda}, \boldsymbol{\xi}), j = 1, \dots, n$ is the error due to that the short-term sub-algorithm only runs for a finite number of J iterations. Suppose that the short-term sub-algorithm converges to a stationary point of $\mathcal{P}_S(\mathbf{x}, \boldsymbol{\lambda}, \boldsymbol{\xi})$ as $J \rightarrow \infty$. Then for all $\mathbf{x} \in \mathcal{X}, \boldsymbol{\lambda} \succeq \mathbf{0}$, we have $\lim_{J \rightarrow \infty} e_i^J(\mathbf{x}, \boldsymbol{\lambda}, \boldsymbol{\xi}) = 0, i = 1, 2, \lim_{J \rightarrow \infty} e_{3,j}^J(\mathbf{x}, \boldsymbol{\lambda}, \boldsymbol{\xi}) = 0, \forall j$. Note that in practice, the short-term sub-algorithm always runs for a finite number of iterations. Therefore, it is meaningful to derive a relaxed primal-dual decomposition theorem for this case.

With the notation of $\mathbf{y}^J(\mathbf{x}, \boldsymbol{\lambda}, \boldsymbol{\xi})$, we formulate the following relaxed long-term problem

$$\begin{aligned} \mathcal{P}_L^J : \min_{\mathbf{x}, \boldsymbol{\lambda}} f_0^J(\mathbf{x}, \boldsymbol{\lambda}) &\triangleq \mathbb{E}[g_0(\mathbf{x}, \mathbf{y}^J(\mathbf{x}, \boldsymbol{\lambda}, \boldsymbol{\xi}), \boldsymbol{\xi})], \quad (14) \\ \text{s.t. } f_i^J(\mathbf{x}, \boldsymbol{\lambda}) &\triangleq \mathbb{E}[g_i(\mathbf{x}, \mathbf{y}^J(\mathbf{x}, \boldsymbol{\lambda}, \boldsymbol{\xi}), \boldsymbol{\xi})] \leq 0, \quad \forall i. \end{aligned}$$

Problem \mathcal{P}_L^J only contains long-term variables $\mathbf{x}, \boldsymbol{\lambda}$. Let $\nabla_{\mathbf{x}} f_i^J(\mathbf{x}, \boldsymbol{\lambda}) \triangleq \mathbb{E}[\partial_{\mathbf{x}} \mathbf{y}^J \partial_{\mathbf{y}} g_i(\mathbf{x}, \mathbf{y}^J, \boldsymbol{\xi}) + \partial_{\mathbf{x}} g_i(\mathbf{x}, \mathbf{y}^J, \boldsymbol{\xi})]$ and $\nabla_{\boldsymbol{\lambda}} f_i^J(\mathbf{x}, \boldsymbol{\lambda}) \triangleq \mathbb{E}[\partial_{\boldsymbol{\lambda}} \mathbf{y}^J \partial_{\mathbf{y}} g_i(\mathbf{x}, \mathbf{y}^J, \boldsymbol{\xi})]$ denote the derivative of $f_i^J(\mathbf{x}, \boldsymbol{\lambda})$ w.r.t. \mathbf{x} and $\boldsymbol{\lambda}$, respectively, where $\partial_{\mathbf{x}} \mathbf{y}^J = \partial_{\mathbf{x}} \mathbf{y}^J(\mathbf{x}, \boldsymbol{\lambda}, \boldsymbol{\xi}) \in \mathbb{R}^{n_x \times n_y}$ ($\partial_{\boldsymbol{\lambda}} \mathbf{y}^J =$

$\partial_{\lambda} \mathbf{y}^J(\mathbf{x}, \boldsymbol{\lambda}, \boldsymbol{\xi}) \in \mathbb{R}^{m \times n_y}$ is the derivative of the vector function $\mathbf{y}^J(\mathbf{x}, \boldsymbol{\lambda}, \boldsymbol{\xi})$ to the vector $\mathbf{x}(\boldsymbol{\lambda})$, \mathbf{y}^J is an abbreviation for $\mathbf{y}^J(\mathbf{x}, \boldsymbol{\lambda}, \boldsymbol{\xi})$. Note that throughout this paper, we use $\nabla_{\mathbf{x}}, \nabla_{\boldsymbol{\lambda}}$ to denote the derivative of f_i^J or g_i by viewing $\mathbf{y}^J(\mathbf{x}, \boldsymbol{\lambda}, \boldsymbol{\xi})$ as a function of $\mathbf{x}, \boldsymbol{\lambda}$, and use $\partial_{\mathbf{x}}, \partial_{\boldsymbol{\lambda}}$ to denote the derivative of f_i^J or g_i by viewing $\mathbf{y}^J(\mathbf{x}, \boldsymbol{\lambda}, \boldsymbol{\xi})$ as a fixed value.

In the following theorem, we establish a relaxed primal-dual decomposition theorem for the two-stage Problem \mathcal{P} , which provides a foundation for the algorithm design.

Theorem 2 (Relaxed Two-stage Primal-Dual Decomposition). *Suppose that for every $\boldsymbol{\xi} \in \Omega$ outside a set of probability zero, $\mathbf{y}^J(\mathbf{x}, \boldsymbol{\lambda}, \boldsymbol{\xi})$ is continuously differentiable function in $\mathbf{x} \in \mathcal{X}$ and $\boldsymbol{\lambda} \succeq \mathbf{0}$. Let $\mathbf{x}^*, \boldsymbol{\lambda}^*$ denote a KKT point of \mathcal{P}_L^J , i.e., there exists Lagrange multipliers $\tilde{\boldsymbol{\lambda}} = [\tilde{\lambda}_1, \dots, \tilde{\lambda}_m]^T \succeq \mathbf{0}$ such that the following KKT conditions are satisfied:*

$$\begin{aligned} \nabla_{\mathbf{x}} f_0^J(\mathbf{x}^*, \boldsymbol{\lambda}^*) + \sum_i \tilde{\lambda}_i \nabla_{\mathbf{x}} f_i^J(\mathbf{x}^*, \boldsymbol{\lambda}^*) &= \mathbf{0}, \\ \nabla_{\boldsymbol{\lambda}} f_0^J(\mathbf{x}^*, \boldsymbol{\lambda}^*) + \sum_i \tilde{\lambda}_i \nabla_{\boldsymbol{\lambda}} f_i^J(\mathbf{x}^*, \boldsymbol{\lambda}^*) &= \mathbf{0}, \\ \tilde{\lambda}_i f_i^J(\mathbf{x}^*, \boldsymbol{\lambda}^*) &= 0, \forall i \\ f_i^J(\mathbf{x}^*, \boldsymbol{\lambda}^*) &\leq 0, \forall i, \end{aligned} \quad (15)$$

Then the primal-dual pair $(\mathbf{x}^* \in \mathcal{X}, \Theta^* = \{\mathbf{y}^J(\mathbf{x}^*, \boldsymbol{\lambda}^*, \boldsymbol{\xi}), \forall \boldsymbol{\xi}\})$ and $\boldsymbol{\lambda}^*$ satisfies the KKT conditions in (8), (9) and (10) up to an error of $O(e(J))$, where $\lim_{J \rightarrow \infty} e(J) = 0$, providing that the following linear independence regularity condition (LIRC) holds: The gradients of the long-term constraints $\nabla_{\boldsymbol{\lambda}} f_i^J(\mathbf{x}^*, \boldsymbol{\lambda}^*), \forall i$ are linearly independent, and the gradients of the short-term constraints $\partial_{\mathbf{y}} h_j(\mathbf{y}^J(\mathbf{x}^*, \boldsymbol{\lambda}^*, \boldsymbol{\xi}), \boldsymbol{\xi}), \forall j$ are also linearly independent for every $\boldsymbol{\xi} \in \Omega$ outside a set of probability zero.

Please refer to Appendix 3 for the proof.

The LIRC in Theorem 2 is used to guarantee the complementary slackness in (10). It is similar to another well known regularity condition, the linear independence constraint qualification (LICQ)¹, in the sense that they both require linear independence conditions on some gradients. However, the details are different, e.g., LICQ requires that the gradients of the active inequality constraints and the gradients of the equality constraints are linearly independent. On the other hand, the condition that $\mathbf{y}^J(\mathbf{x}, \boldsymbol{\lambda}, \boldsymbol{\xi})$ is continuously differentiable can be guaranteed by the short-term sub-algorithm design, as will be detailed in Section IV-B.

IV. PRIMAL-DUAL DECOMPOSITION BASED STOCHASTIC SUCCESSIVE CONVEX APPROXIMATION

Theorem 2 states that a KKT solution (up to error $e(J)$) can be found by first solving a stationary point $\mathbf{x}^*, \boldsymbol{\lambda}^*$ of the relaxed long-term problem \mathcal{P}_L^J , and then finding a stationary point $\mathbf{y}^J(\mathbf{x}, \boldsymbol{\lambda}, \boldsymbol{\xi})$ of $\mathcal{P}_S(\mathbf{x}^*, \boldsymbol{\lambda}^*, \boldsymbol{\xi})$ for each $\boldsymbol{\xi}$. In this section,

we propose PDD-SSCA to find KKT solutions of \mathcal{P} . Specifically, PDD-SSCA contains two sub-algorithms: a long-term sub-algorithm and a short-term sub-algorithm. We first present the long-term sub-algorithm which converges to a stationary point of the non-convex constrained stochastic optimization problem \mathcal{P}_L^J . Then, we discuss several general methods to design the short-term sub-algorithm that finds a stationary point of $\mathcal{P}_S(\mathbf{x}, \boldsymbol{\lambda}, \boldsymbol{\xi})$. Finally, we establish the convergence of the overall algorithm. The implementation details for the overall algorithm are provided in Section V.

A. Long-term Sub-Algorithm for \mathcal{P}_L^J

The long-term problem \mathcal{P}_L^J is a single-stage stochastic optimization problem with non-convex constraints. The conventional single-stage stochastic SCA algorithms in [24], [25] only consider deterministic and convex constraints. Recently, a constrained stochastic successive convex approximation (CSSCA) framework is proposed in [26] to find a stationary point for a non-convex constrained single-stage stochastic optimization problem. The long-term sub-algorithm in this paper is based on the CSSCA framework and is summarized in Algorithm 1. In the t -th iteration, the long-term variables $\mathbf{x}, \boldsymbol{\lambda}$ are updated by solving a convex optimization problem obtained by replacing the objective and constraint functions $f_i^J(\mathbf{x}, \boldsymbol{\lambda}), i = 0, 1, \dots, m$ with their convex surrogate functions $\bar{f}_i^t(\mathbf{x}, \boldsymbol{\lambda}), i = 0, 1, \dots, m$, as elaborated below.

In Step 1 of the t -th iteration, one random mini-batch $\{\boldsymbol{\xi}_j^t, j = 1, \dots, B\}$ of B state samples are obtained and the surrogate functions $\bar{f}_i^t(\mathbf{x}, \boldsymbol{\lambda})$ are constructed based on the mini-batch $\{\boldsymbol{\xi}_j^t\}$ and the current iterate $\mathbf{x}^t, \boldsymbol{\lambda}^t$. The surrogate functions $\bar{f}_i^t(\mathbf{x}, \boldsymbol{\lambda})$ can be viewed as convex approximations of the objective and constraint functions $f_i^J(\mathbf{x}, \boldsymbol{\lambda}), \forall i$ of the long-term problem \mathcal{P}_L^J . Specifically, divide $g_i(\mathbf{x}, \mathbf{y}, \boldsymbol{\xi})$ into two components as

$$g_i(\mathbf{x}, \mathbf{y}, \boldsymbol{\xi}) = g_i^c(\mathbf{x}, \mathbf{y}, \boldsymbol{\xi}) + g_i^{\bar{c}}(\mathbf{x}, \mathbf{y}, \boldsymbol{\xi}),$$

such that $g_i^c(\mathbf{x}, \mathbf{y}, \boldsymbol{\xi})$ is convex w.r.t. \mathbf{x} and $g_i^{\bar{c}}(\mathbf{x}, \mathbf{y}, \boldsymbol{\xi})$ can be either convex or non-convex. Then a structured surrogate function $\bar{f}_i^t(\mathbf{x}, \boldsymbol{\lambda})$ can be constructed as [26]

$$\begin{aligned} \bar{f}_i^t(\mathbf{x}, \boldsymbol{\lambda}) &= (1 - \rho^t) f_i^{t-1} + \rho^t \frac{1}{B} \sum_{j=1}^B \left[g_i^c(\mathbf{x}, \mathbf{y}_j^t, \boldsymbol{\xi}_j^t) \right. \\ &\quad \left. + g_i^{\bar{c}}(\mathbf{x}^t, \mathbf{y}_j^t, \boldsymbol{\xi}_j^t) + \partial_{\mathbf{x}}^T g_i^{\bar{c}}(\mathbf{x}^t, \mathbf{y}_j^t, \boldsymbol{\xi}_j^t) (\mathbf{x} - \mathbf{x}^t) \right] \\ &\quad + ((1 - \rho^t) \mathbf{f}_{x,i}^{t-1} + \mathbf{f}_{y,i}^t)^T (\mathbf{x} - \mathbf{x}^t) \\ &\quad + (\mathbf{f}_{\lambda,i}^t)^T (\boldsymbol{\lambda} - \boldsymbol{\lambda}^t) + \tau_i (\|\mathbf{x} - \mathbf{x}^t\|^2 + \|\boldsymbol{\lambda} - \boldsymbol{\lambda}^t\|^2), \end{aligned} \quad (16)$$

where \mathbf{y}_j^t is an abbreviation for $\mathbf{y}^J(\mathbf{x}^t, \boldsymbol{\lambda}^t, \boldsymbol{\xi}_j^t)$, $\{\rho^t \in (0, 1]\}$ is a decreasing sequence satisfying $\rho^t \rightarrow 0, \sum_t \rho^t = \infty, \sum_t (\rho^t)^2 < \infty, \tau_i > 0$ can be any constant, \bar{f}_i^t is an approximation for $f_i^J(\mathbf{x}^t, \boldsymbol{\lambda}^t)$ and it is updated recursively according to

$$\bar{f}_i^t = (1 - \rho^t) \bar{f}_i^{t-1} + \rho^t \frac{1}{B} \sum_{j=1}^B g_i(\mathbf{x}^t, \mathbf{y}_j^t, \boldsymbol{\xi}_j^t),$$

¹LICQ ensures the existence of KKT point (i.e., stationary point that satisfies KKT conditions) for a smooth optimization problem.

with $f_i^{-1} = 0$, and $\mathbf{f}_{x,i}^t, \mathbf{f}_{y,i}^t, \mathbf{f}_{\lambda,i}^t$ are approximations for the gradients $\mathbb{E}[\partial_{\mathbf{x}} g_i(\mathbf{x}, \mathbf{y}^J(\mathbf{x}, \boldsymbol{\lambda}, \boldsymbol{\xi}), \boldsymbol{\xi})]$, $\mathbb{E}[\partial_{\mathbf{x}} \mathbf{y}^J(\mathbf{x}, \boldsymbol{\lambda}, \boldsymbol{\xi}) \partial_{\mathbf{y}} g_i(\mathbf{x}, \mathbf{y}^J(\mathbf{x}, \boldsymbol{\lambda}, \boldsymbol{\xi}), \boldsymbol{\xi})]$ and $\mathbb{E}[\nabla_{\boldsymbol{\lambda}} g_i(\mathbf{x}, \mathbf{y}^J(\mathbf{x}, \boldsymbol{\lambda}, \boldsymbol{\xi}), \boldsymbol{\xi})]$, respectively, which are updated recursively according to

$$\begin{aligned} \mathbf{f}_{x,i}^t &= (1 - \rho^t) \mathbf{f}_{x,i}^{t-1} + \rho^t \frac{1}{B} \sum_{j=1}^B \partial_{\mathbf{x}} g_i(\mathbf{x}^t, \mathbf{y}_j^t, \boldsymbol{\xi}_j^t), \\ \mathbf{f}_{y,i}^t &= (1 - \rho^t) \mathbf{f}_{y,i}^{t-1} + \rho^t \frac{1}{B} \sum_{j=1}^B \partial_{\mathbf{x}} \mathbf{y}_j^t \partial_{\mathbf{y}} g_i(\mathbf{x}^t, \mathbf{y}_j^t, \boldsymbol{\xi}_j^t), \\ \mathbf{f}_{\lambda,i}^t &= (1 - \rho^t) \mathbf{f}_{\lambda,i}^{t-1} + \rho^t \frac{1}{B} \sum_{j=1}^B \partial_{\boldsymbol{\lambda}} \mathbf{y}_j^t \partial_{\mathbf{y}} g_i(\mathbf{x}^t, \mathbf{y}_j^t, \boldsymbol{\xi}_j^t), \end{aligned} \quad (17)$$

with $\mathbf{f}_i^{-1} = \mathbf{0}$, $\partial_{\mathbf{x}} \mathbf{y}_j^t = \partial_{\mathbf{x}} \mathbf{y}^J(\mathbf{x}^t, \boldsymbol{\lambda}^t, \boldsymbol{\xi}_j^t) \in \mathbb{R}^{n_x \times n_y}$ ($\partial_{\boldsymbol{\lambda}} \mathbf{y}_j^t = \partial_{\boldsymbol{\lambda}} \mathbf{y}^J(\mathbf{x}^t, \boldsymbol{\lambda}^t, \boldsymbol{\xi}_j^t) \in \mathbb{R}^{m \times n_y}$) is the derivative of the vector function $\mathbf{y}^J(\mathbf{x}^t, \boldsymbol{\lambda}^t, \boldsymbol{\xi}_j^t)$ to the vector $\mathbf{x}(\boldsymbol{\lambda})$. Later in Lemma 1, we will show that $\lim_{t \rightarrow \infty} f_i^t - f_i^J(\mathbf{x}^t, \boldsymbol{\lambda}^t) = 0$, $\lim_{t \rightarrow \infty} \mathbf{f}_{x,i}^t + \mathbf{f}_{y,i}^t - \nabla_{\mathbf{x}} f_i^J(\mathbf{x}^t, \boldsymbol{\lambda}^t) = \mathbf{0}$ and $\lim_{t \rightarrow \infty} \mathbf{f}_{\lambda,i}^t - \nabla_{\boldsymbol{\lambda}} f_i^J(\mathbf{x}^t, \boldsymbol{\lambda}^t) = \mathbf{0}$. Therefore, the function value and gradient of $f_i^t(\mathbf{x}, \boldsymbol{\lambda})$ is consistent with that of the original function $f_i^J(\mathbf{x}, \boldsymbol{\lambda})$ at the current iterate $\mathbf{x}^t, \boldsymbol{\lambda}^t$, which is the key to guarantee the convergence of the algorithm to a stationary point. The structured surrogate function in (16) contains the convex component $g_i^c(\mathbf{x}, \mathbf{y}_j^t, \boldsymbol{\xi}_j^t)$ of the original sample objective function $g_i(\mathbf{x}, \mathbf{y}_j^t, \boldsymbol{\xi}_j^t)$, which may help to reduce the approximation error and potentially achieve a faster initial convergence speed [25]. How to divide $g_i(\mathbf{x}, \mathbf{y}, \boldsymbol{\xi})$ into two components to achieve a good initial convergence speed depends on the specific problem.

In Step 2 of the t -th iteration, the optimal solution $\bar{\mathbf{x}}^t, \bar{\boldsymbol{\lambda}}^t$ of the following problem is solved:

$$\begin{aligned} (\bar{\mathbf{x}}^t, \bar{\boldsymbol{\lambda}}^t) &= \underset{\mathbf{x} \in \mathcal{X}, \boldsymbol{\lambda} \succeq \mathbf{0}}{\operatorname{argmin}} \bar{f}_0^t(\mathbf{x}, \boldsymbol{\lambda}) \\ \text{s.t. } \bar{f}_i^t(\mathbf{x}, \boldsymbol{\lambda}) &\leq 0, \forall i, \end{aligned} \quad (18)$$

which is a convex approximation of \mathcal{P}_L^J . Note that Problem (18) is not necessarily feasible. If Problem (18) turns out to be infeasible, the optimal solution $(\bar{\mathbf{x}}^t, \bar{\boldsymbol{\lambda}}^t)$ of the following convex problem is solved:

$$\begin{aligned} (\bar{\mathbf{x}}^t, \bar{\boldsymbol{\lambda}}^t) &= \underset{\mathbf{x} \in \mathcal{X}, \boldsymbol{\lambda} \succeq \mathbf{0}, \alpha}{\operatorname{argmin}} \alpha \\ \text{s.t. } \bar{f}_i^t(\mathbf{x}) &\leq \alpha, \forall i, \end{aligned} \quad (19)$$

which minimizes the approximate constraint functions.

Finally, in Step 3, given $\bar{\mathbf{x}}^t, \bar{\boldsymbol{\lambda}}^t$ in one of the above two cases, $\mathbf{x}, \boldsymbol{\lambda}$ is updated according to

$$\begin{aligned} \mathbf{x}^{t+1} &= (1 - \gamma^t) \mathbf{x}^t + \gamma^t \bar{\mathbf{x}}^t, \\ \boldsymbol{\lambda}^{t+1} &= (1 - \gamma^t) \boldsymbol{\lambda}^t + \gamma^t \bar{\boldsymbol{\lambda}}^t. \end{aligned} \quad (20)$$

where $\{\gamma^t \in (0, 1]\}$ is a decreasing sequence satisfying $\gamma^t \rightarrow 0$, $\sum_t \gamma^t = \infty$, $\sum_t (\gamma^t)^2 < \infty$, $\lim_{t \rightarrow \infty} \gamma^t / \rho^t = 0$.

Algorithm 1 Long-term Sub-Algorithm for \mathcal{P}_L^J

Input: $\{\rho^t, \gamma^t\}$.

Initialize: $\mathbf{x}^0 \in \mathcal{X}, \boldsymbol{\lambda}^0 \succeq \mathbf{0}; t = 0$.

Step 1:

Obtain a mini-batch $\{\boldsymbol{\xi}_j^t, j = 1, \dots, B\}$.

Construct the surrogate functions $\bar{f}_i^t(\mathbf{x}, \boldsymbol{\lambda}), \forall i$ according to (16).

Step 2:

//Objective update

If Problem (18) is feasible
Solve (18) to obtain $\bar{\mathbf{x}}^t, \bar{\boldsymbol{\lambda}}^t$.

//Feasible update

Else

Solve (19) to obtain $\bar{\mathbf{x}}^t, \bar{\boldsymbol{\lambda}}^t$.

End if

Step 3:

Update $\mathbf{x}^{t+1}, \boldsymbol{\lambda}^{t+1}$ according to (20).

Step 4:

Let $t = t + 1$ and return to Step 1.

B. Short-term Sub-Algorithm for \mathcal{P}_S

The short-term subproblem $\mathcal{P}_S(\mathbf{x}, \boldsymbol{\lambda}, \boldsymbol{\xi})$ can be solved using existing deterministic optimization algorithms. In general, a deterministic and iterative short-term sub-algorithm starts from an initial point $\mathbf{y}^0(\mathbf{x}, \boldsymbol{\lambda}, \boldsymbol{\xi})$, and then generates a sequence $\{\mathbf{y}^j(\mathbf{x}, \boldsymbol{\lambda}, \boldsymbol{\xi})\}$ of iterates that converge to a stationary point of the short-term subproblem $\mathcal{P}_S(\mathbf{x}, \boldsymbol{\lambda}, \boldsymbol{\xi})$. Specifically, the j -th iteration of a general short-term sub-algorithm can be expressed as a mapping from $\mathbf{y}^{j-1}(\mathbf{x}, \boldsymbol{\lambda}, \boldsymbol{\xi})$ to $\mathbf{y}^j(\mathbf{x}, \boldsymbol{\lambda}, \boldsymbol{\xi})$ as

$$\mathbf{y}^j(\mathbf{x}, \boldsymbol{\lambda}, \boldsymbol{\xi}) = \mathcal{A}^j(\mathbf{y}^{j-1}(\mathbf{x}, \boldsymbol{\lambda}, \boldsymbol{\xi}), \mathbf{x}, \boldsymbol{\lambda}, \boldsymbol{\xi}), j = 1, 2, \dots, \quad (21)$$

which depends on problem parameters $\mathbf{x}, \boldsymbol{\lambda}, \boldsymbol{\xi}$.

To avoid confusion with the iteration of the long-term sub-algorithm, an iteration of the short-term sub-algorithm will be called an *inner iteration*. To ensure the convergence of the overall algorithm, the short-term sub-algorithm is assumed to satisfy the following conditions.

Assumption 2 (Assumptions on the short-term sub-algorithm).

- 1) The initial point $\mathbf{y}^0(\mathbf{x}, \boldsymbol{\lambda}, \boldsymbol{\xi})$ is differentiable w.r.t. $\mathbf{x}, \boldsymbol{\lambda}$, w.p.1.
- 2) For any $\mathbf{x} \in \mathcal{X}, \mathbf{y} \in \mathcal{Y}, \boldsymbol{\lambda} \succeq \mathbf{0}$ and iteration number j , $\mathcal{A}^j(\mathbf{y}, \mathbf{x}, \boldsymbol{\lambda}, \boldsymbol{\xi})$ is differentiable w.r.t. $\mathbf{y}, \mathbf{x}, \boldsymbol{\lambda}$, w.p.1.
- 3) For any $\mathbf{x} \in \mathcal{X}, \boldsymbol{\lambda} \succeq \mathbf{0}$, the sequence $\{\mathbf{y}^j(\mathbf{x}, \boldsymbol{\lambda}, \boldsymbol{\xi})\}$ converges to a stationary set of $\mathcal{P}_S(\mathbf{x}, \boldsymbol{\lambda}, \boldsymbol{\xi})$, w.p.1.

Assumption 2 ensures that $\mathbf{y}^j(\mathbf{x}, \boldsymbol{\lambda}, \boldsymbol{\xi})$ is differentiable w.r.t. $\mathbf{x}, \boldsymbol{\lambda}$ for any finite J and $\mathbf{y}^J(\mathbf{x}, \boldsymbol{\lambda}, \boldsymbol{\xi})$ satisfies the KKT conditions of $\mathcal{P}_S(\mathbf{x}, \boldsymbol{\lambda}, \boldsymbol{\xi})$ (up to certain tolerable error $O(e(J))$) as in (13). The first condition in Assumption 2 can be satisfied by a proper choice of the initial points $\mathbf{y}^0(\mathbf{x}, \boldsymbol{\lambda}, \boldsymbol{\xi}), \forall \mathbf{x}, \boldsymbol{\lambda}, \boldsymbol{\xi}$. The second and third conditions are satisfied by many standard iterative algorithms that are designed to find stationary points of a non-convex problem. In the following, we give two examples of short-term sub-algorithms that satisfy Assumption 2.

1) *Gradient Projection Algorithm*: When the feasible set of the short-term subproblem $\mathcal{P}_S(\mathbf{x}, \boldsymbol{\lambda}, \boldsymbol{\xi})$, denoted by $\mathcal{Y}(\mathbf{x}, \boldsymbol{\lambda}, \boldsymbol{\xi}) \triangleq \{\mathbf{y} \in \mathcal{Y} : h_j(\mathbf{y}(\boldsymbol{\xi}), \boldsymbol{\xi}) \leq 0, \forall j\}$, is convex, the gradient projection (GP) algorithm [27] can be used to find a stationary point of $\mathcal{P}_S(\mathbf{x}, \boldsymbol{\lambda}, \boldsymbol{\xi})$. Note that the objective function of $\mathcal{P}_S(\mathbf{x}, \boldsymbol{\lambda}, \boldsymbol{\xi})$ can still be non-convex. When the GP algorithm is used as the short-term sub-algorithm, the mapping $\mathcal{A}^j(\mathbf{y}^{j-1}(\mathbf{x}, \boldsymbol{\lambda}, \boldsymbol{\xi}), \mathbf{x}, \boldsymbol{\lambda}, \boldsymbol{\xi})$ for the j -th inner iteration is given by

$$\mathcal{A}^j(\mathbf{y}^{j-1}) = \mathbb{P}_{\mathcal{Y}(\mathbf{x}, \boldsymbol{\lambda}, \boldsymbol{\xi})} [\mathbf{y}^{j-1} - \alpha_j \partial_{\mathbf{y}} g_s(\mathbf{x}, \boldsymbol{\lambda}, \mathbf{y}^{j-1}, \boldsymbol{\xi})], \quad (22)$$

where $g_s(\mathbf{x}, \boldsymbol{\lambda}, \mathbf{y}, \boldsymbol{\xi}) = g_0(\mathbf{x}, \mathbf{y}, \boldsymbol{\xi}) + \sum_i \lambda_i g_i(\mathbf{x}, \mathbf{y}, \boldsymbol{\xi})$, $\mathbb{P}_{\mathcal{Y}(\mathbf{x}, \boldsymbol{\lambda}, \boldsymbol{\xi})}$ is the projection onto the feasible set $\mathcal{Y}(\mathbf{x}, \boldsymbol{\lambda}, \boldsymbol{\xi})$, and $\{\alpha_j > 0, j = 1, \dots, J\}$ is a properly chosen step size sequence, e.g., a diminishing step size sequence [27]. Note that we have omitted $(\mathbf{x}, \boldsymbol{\lambda}, \boldsymbol{\xi})$ in the mapping \mathcal{A}^j for simplicity of notation. It can be verified that the GP algorithm satisfies Assumption 2.

2) *Majorization-Minimization Algorithm*: Majorization-Minimization (MM) [8], [28] can be used to find a stationary point of $\mathcal{P}_S(\mathbf{x}, \boldsymbol{\lambda}, \boldsymbol{\xi})$ for general cases. When MM is used as the short-term sub-algorithm, the mapping $\mathcal{A}^j(\mathbf{y}^{j-1}(\mathbf{x}, \boldsymbol{\xi}), \mathbf{x}, \boldsymbol{\lambda}, \boldsymbol{\xi})$ is given by

$$\begin{aligned} \mathcal{A}^j(\mathbf{y}^{j-1}) = & \underset{\mathbf{y}}{\operatorname{argmin}} u_s(\mathbf{y}; \mathbf{y}^{j-1}, \mathbf{x}, \boldsymbol{\lambda}) \\ \text{s.t. } & u_i(\mathbf{y}; \mathbf{y}^{j-1}) \leq 0, i = 1, \dots, n, \end{aligned} \quad (23)$$

where $u_s(\mathbf{y}; \mathbf{y}^{j-1}, \mathbf{x}, \boldsymbol{\lambda})$ is a surrogate function of $g_s(\mathbf{x}, \boldsymbol{\lambda}, \mathbf{y}, \boldsymbol{\xi})$, $u_i(\mathbf{y}; \mathbf{y}^{j-1})$ is a surrogate function of $h_i(\mathbf{y}, \boldsymbol{\xi})$ for $i = 1, \dots, n$, satisfying the following conditions:

- 1) $u_s(\mathbf{y}^{j-1}; \mathbf{y}^{j-1}, \mathbf{x}, \boldsymbol{\lambda}) = g_s(\mathbf{x}, \boldsymbol{\lambda}, \mathbf{y}^{j-1}, \boldsymbol{\xi})$, $u_s(\mathbf{y}; \mathbf{y}^{j-1}, \mathbf{x}, \boldsymbol{\lambda}) \geq g_s(\mathbf{x}, \boldsymbol{\lambda}, \mathbf{y}, \boldsymbol{\xi}), \forall \mathbf{y} \in \mathcal{Y}$ and $\nabla u_s(\mathbf{y}^{j-1}; \mathbf{y}^{j-1}, \mathbf{x}, \boldsymbol{\lambda}) = \partial_{\mathbf{y}} g_s(\mathbf{x}, \boldsymbol{\lambda}, \mathbf{y}^{j-1}, \boldsymbol{\xi})$.
- 2) $u_i(\mathbf{y}^{j-1}; \mathbf{y}^{j-1}) = h_i(\mathbf{y}^{j-1}, \boldsymbol{\xi})$, $u_i(\mathbf{y}; \mathbf{y}^{j-1}) \geq h_i(\mathbf{y}, \boldsymbol{\xi}), \forall \mathbf{y} \in \mathcal{Y}$ and $\nabla u_i(\mathbf{y}^{j-1}; \mathbf{y}^{j-1}) = \partial_{\mathbf{y}} h_i(\mathbf{y}^{j-1}, \boldsymbol{\xi})$.
- 3) $u_i(\mathbf{y}; \mathbf{y}^{j-1})$ is uniformly strongly convex in \mathbf{y} .
- 4) $u_s(\mathbf{y}; \mathbf{y}', \mathbf{x}, \boldsymbol{\lambda})$ and $u_i(\mathbf{y}; \mathbf{y}')$, $\forall i$ are differentiable w.r.t. $\mathbf{y}', \mathbf{y}, \mathbf{x}, \boldsymbol{\lambda}$.

A simple example surrogate function that satisfies the above four conditions is

$$\begin{aligned} u_s(\mathbf{y}; \mathbf{y}', \mathbf{x}, \boldsymbol{\lambda}) = & g_s(\mathbf{x}, \boldsymbol{\lambda}, \mathbf{y}', \boldsymbol{\xi}) + \tau_s \left\| \mathbf{y} - \mathbf{y}' \right\|^2 \\ & + \partial_{\mathbf{y}}^T g_s(\mathbf{x}, \boldsymbol{\lambda}, \mathbf{y}', \boldsymbol{\xi}) (\mathbf{y} - \mathbf{y}'), \end{aligned}$$

$$\begin{aligned} u_i(\mathbf{y}; \mathbf{y}') = & h_i(\mathbf{y}', \boldsymbol{\xi}) + \partial_{\mathbf{y}}^T h_i(\mathbf{y}', \boldsymbol{\xi}) (\mathbf{y} - \mathbf{y}') \\ & + \tau_{s,i} \left\| \mathbf{y} - \mathbf{y}' \right\|^2, \end{aligned}$$

where $\tau_s, \tau_{s,i} > 0$ is chosen to be a sufficiently large number to satisfy the upper bound condition: $u_s(\mathbf{y}; \mathbf{y}^{j-1}, \mathbf{x}, \boldsymbol{\lambda}) \geq g_s(\mathbf{x}, \boldsymbol{\lambda}, \mathbf{y}, \boldsymbol{\xi}), \forall \mathbf{y} \in \mathcal{Y}$ and $u_i(\mathbf{y}; \mathbf{y}^{j-1}) \geq h_i(\mathbf{y}, \boldsymbol{\xi}), \forall \mathbf{y} \in \mathcal{Y}$. Note that such $\tau_s, \tau_{s,i}$ can always be found since the second-order derivative of the functions $g_s(\mathbf{x}, \boldsymbol{\lambda}, \mathbf{y}, \boldsymbol{\xi})$ and $h_i(\mathbf{y}, \boldsymbol{\xi})$'s are assumed to be uniformly bounded.

From the convergence result for the MM algorithm in [28] and the above conditions on $u_s(\mathbf{y}; \mathbf{y}^{j-1}, \mathbf{x}, \boldsymbol{\lambda})$ and $u_i(\mathbf{y}; \mathbf{y}^{j-1}), \forall i$, one can verify that the MM algorithm satisfies Assumption 2.

3) *Short-term Sub-Algorithm for Section II-B*: In this subsection, we give concrete examples of the short-term sub-algorithm for our applications in Section II-B.

In Example 1, the short-term subproblem $\mathcal{P}_S(\boldsymbol{\lambda}, \Upsilon, \mathbf{a}, \mathbf{b})$ is given by

$$\begin{aligned} \min - & \left[\log \left(1 + \sum_{i=1}^N a_i p_i \right) \right] + \sum_{i=1}^N \lambda_i p_i + \Upsilon \sum_{i=1}^N b_i p_i, \\ \text{s.t. } & \Upsilon \geq 0, \lambda_i \geq 0, p_i \geq 0, i = 1, \dots, N, \end{aligned} \quad (24)$$

where λ_i and Υ are the long-term Lagrange multipliers associated with the long-term transmit power budget at SU i and the interference threshold constraint for the PU, respectively. The optimal solution of $\mathcal{P}_S(\boldsymbol{\lambda}, \Upsilon, \mathbf{a}, \mathbf{b})$ has a closed-form expression given by

$$p_i^*(\boldsymbol{\lambda}, \Upsilon, \mathbf{a}, \mathbf{b}) = \frac{1}{N a_i} \left(\frac{a_i}{b_i \Upsilon + \lambda_i} - 1 \right)^+. \quad (25)$$

In Example 2, the short-term subproblem $\mathcal{P}_S(\boldsymbol{\theta}, \boldsymbol{\lambda}, \mathbf{H})$ is given by

$$\min_{\mathbf{G}} \operatorname{Tr}(\mathbf{F} \mathbf{G} \mathbf{G}^H \mathbf{F}^H) - \sum_{k=1}^K \lambda_k r_k(\boldsymbol{\theta}, \mathbf{G}, \mathbf{H}), \quad (26)$$

where $\boldsymbol{\lambda} = [\lambda_1, \dots, \lambda_K]$ are the Lagrange multipliers associated with the average rate constraints. A stationary point of $\mathcal{P}_S(\boldsymbol{\theta}, \boldsymbol{\lambda}, \mathbf{H})$ can be found using the WMMSE algorithm [29]. The basic idea is to first transform $\mathcal{P}_S(\boldsymbol{\theta}, \boldsymbol{\lambda}, \mathbf{H})$ into the following WMMSE problem by introducing two auxiliary variables \mathbf{w}, \mathbf{u} :

$$\min_{\{\mathbf{w}, \mathbf{u}, \mathbf{G}\}} \operatorname{Tr}(\mathbf{F} \mathbf{G} \mathbf{G}^H \mathbf{F}^H) + \sum_{k=1}^K \lambda_k (w_k e_k - \log w_k), \quad (27)$$

where $\mathbf{w} = [w_1, \dots, w_K]^T$ with $w_k > 0 : \forall k$ is a weight vector for MSE; $\mathbf{u} = [u_1, \dots, u_K]^T$ with u_k denoting the receive coefficient; and

$$e_k \triangleq \left| u_k^* \mathbf{h}_k^H \mathbf{F} \mathbf{g}_k - 1 \right|^2 + \sum_{i \neq k} \left| u_k^* \mathbf{h}_k^H \mathbf{F} \mathbf{g}_i \right|^2 + |u_k|^2, \quad (28)$$

is the MSE of user k . Problem (27) is convex in each of the optimization variables $\mathbf{w}, \mathbf{u}, \mathbf{G}$. Then, we can use the block coordinate descent method to solve (27). Specifically, for given \mathbf{G} , the optimal \mathbf{u} is given by the MMSE receive coefficient:

$$u_k = \left(\sum_{i=1}^K \left| \mathbf{h}_k^H \mathbf{F} \mathbf{g}_i \right|^2 + 1 \right)^{-1} \mathbf{h}_k^H \mathbf{F} \mathbf{g}_k, \forall k. \quad (29)$$

For given \mathbf{G}, \mathbf{u} , the optimal \mathbf{w} is given by

$$w_k = \left(1 - u_k^* \mathbf{h}_k^H \mathbf{F} \mathbf{g}_k \right)^{-1}, \forall k. \quad (30)$$

Finally, for given \mathbf{w}, \mathbf{u} , the optimal $\mathbf{G} = [\mathbf{g}_1, \dots, \mathbf{g}_K]$ is given by

$$\mathbf{g}_k = \left(\lambda_k w_k \sum_{i=1}^K |u_i|^2 \mathbf{F}^H \mathbf{h}_i \mathbf{h}_i^H \mathbf{F} + \mathbf{I} \right)^{-1} \lambda_k w_k u_k \mathbf{F}^H \mathbf{h}_k. \quad (31)$$

After running (29) to (31) for J iterations, we obtain an approximate stationary point of $\mathcal{P}_S(\boldsymbol{\theta}, \boldsymbol{\lambda}, \mathbf{H})$ denoted as $\mathbf{G}^J(\boldsymbol{\theta}, \boldsymbol{\lambda}, \mathbf{H})$.

C. Overall Algorithm and Convergence Analysis

In this section, we first describe the overall PDD-SSCA algorithm. Then we analyze the convergence of the PDD-SSCA algorithm. The PDD-SSCA algorithm first runs the long-term sub-algorithm to find a stationary point of the long-term sub-problem $\mathbf{x}^*, \boldsymbol{\lambda}^*$, and then runs the short-term sub-algorithm to find a stationary point $\mathbf{y}^J(\mathbf{x}^*, \boldsymbol{\lambda}^*, \boldsymbol{\xi})$ of the short-term problem $\mathcal{P}_S(\mathbf{x}^*, \boldsymbol{\lambda}^*, \boldsymbol{\xi})$ for each state realization $\boldsymbol{\xi}$ with fixed $\mathbf{x}^*, \boldsymbol{\lambda}^*$. In the following, we will show that the solution $(\mathbf{x}^*, \Theta^* = \{\mathbf{y}^J(\mathbf{x}^*, \boldsymbol{\lambda}^*, \boldsymbol{\xi}), \forall \boldsymbol{\xi}\})$ found by the PDD-SSCA algorithm is a KKT solution of the original two-stage stochastic optimization problem \mathcal{P} .

We first prove a key Lemma which establishes several important properties of the surrogate functions $\bar{f}_i^t(\mathbf{x}, \boldsymbol{\lambda})$'s.

Lemma 1 (Properties of surrogate functions). *For all $i \in \{0, \dots, m\}$ and $t = 0, 1, \dots$, we have*

- 1) $\bar{f}_i^t(\mathbf{x}, \boldsymbol{\lambda})$ is uniformly strongly convex in $\mathbf{x}, \boldsymbol{\lambda}$.
- 2) $\bar{f}_i^t(\mathbf{x}, \boldsymbol{\lambda})$ is a Lipschitz continuous function w.r.t. $\mathbf{x}, \boldsymbol{\lambda}$. Moreover, $\limsup_{t_1, t_2 \rightarrow \infty} |\bar{f}_i^{t_1}(\mathbf{x}, \boldsymbol{\lambda}) - \bar{f}_i^{t_2}(\mathbf{x}, \boldsymbol{\lambda})| - B\sqrt{\|\mathbf{x}^{t_1} - \mathbf{x}^{t_2}\|^2 + \|\boldsymbol{\lambda}^{t_1} - \boldsymbol{\lambda}^{t_2}\|^2} \leq 0, \forall \mathbf{x} \in \mathcal{X}, \boldsymbol{\lambda} \succeq \mathbf{0}$ for some constant $B > 0$.
- 3) For any $\mathbf{x} \in \mathcal{X}, \boldsymbol{\lambda} \succeq \mathbf{0}$, the function $\bar{f}_i^t(\mathbf{x}, \boldsymbol{\lambda})$, its derivative, and its second order derivative are uniformly bounded.
- 4) $\lim_{t \rightarrow \infty} \left| \bar{f}_i^t(\mathbf{x}^t, \boldsymbol{\lambda}^t) - f_i^J(\mathbf{x}^t, \boldsymbol{\lambda}^t) \right| = 0$, $\lim_{t \rightarrow \infty} \left\| \nabla_{\mathbf{x}} \bar{f}_i^t(\mathbf{x}^t, \boldsymbol{\lambda}^t) - \nabla_{\mathbf{x}} f_i^J(\mathbf{x}^t, \boldsymbol{\lambda}^t) \right\| = 0$ and $\lim_{t \rightarrow \infty} \left\| \nabla_{\boldsymbol{\lambda}} \bar{f}_i^t(\mathbf{x}^t, \boldsymbol{\lambda}^t) - \nabla_{\boldsymbol{\lambda}} f_i^J(\mathbf{x}^t, \boldsymbol{\lambda}^t) \right\| = 0$.
- 5) Consider a subsequence $\{\mathbf{x}^{t_j}, \boldsymbol{\lambda}^{t_j}\}_{j=1}^{\infty}$ converging to a limit point $(\mathbf{x}^*, \boldsymbol{\lambda}^*)$. There exist uniformly differentiable functions $\hat{f}_i(\mathbf{x}, \boldsymbol{\lambda})$ such that

$$\lim_{j \rightarrow \infty} \bar{f}_i^{t_j}(\mathbf{x}, \boldsymbol{\lambda}) = \hat{f}_i(\mathbf{x}, \boldsymbol{\lambda}), \quad \forall \mathbf{x} \in \mathcal{X}, \boldsymbol{\lambda} \succeq \mathbf{0}, \quad (32)$$

almost surely.

Please refer to Appendix 1 for the proof.

The convergence analysis also relies on the Slater condition defined below.

Slater condition: Given a subsequence $\{\mathbf{x}^{t_j}, \boldsymbol{\lambda}^{t_j}\}_{j=1}^{\infty}$ converging to a limit point $(\mathbf{x}^*, \boldsymbol{\lambda}^*)$ and let $\hat{f}_i(\mathbf{x}, \boldsymbol{\lambda}), \forall i$ be the converged surrogate functions as defined in Lemma 1. We say that the Slater condition is satisfied at $(\mathbf{x}^*, \boldsymbol{\lambda}^*)$ if there exists $(\mathbf{x}^*, \boldsymbol{\lambda}^*) \in \text{relint} \mathcal{X} \times \mathbb{R}^{++}$ such that

$$\hat{f}_i(\mathbf{x}^*, \boldsymbol{\lambda}^*) < 0, \quad \forall i = 1, \dots, m.$$

With Lemma 1 and the Slater condition, we are ready to prove the following main convergence result.

Theorem 3 (Convergence of Algorithm 1). *Suppose Assumptions 1 and 2 are satisfied, and the initial point $\mathbf{x}^0 \in \mathcal{X}, \boldsymbol{\lambda}^0 \in \mathbb{R}^{++}$ is a feasible point, i.e., $\max_{i \in \{1, \dots, m\}} f_i^J(\mathbf{x}^0, \boldsymbol{\lambda}^0) \leq 0$. Let $\{\mathbf{x}^t, \boldsymbol{\lambda}^t\}_{t=1}^{\infty}$ denote the iterates generated by Algorithm 1 with a sufficiently small initial step size γ^0 . Then every limiting point $(\mathbf{x}^*, \boldsymbol{\lambda}^*)$ of $\{\mathbf{x}^t, \boldsymbol{\lambda}^t\}_{t=1}^{\infty}$ satisfying the LIRC in Theorem 2 and the Slater condition, almost surely satisfies the KKT conditions in (8), (9) and (10) up to an error of $O(e(J))$, where $\lim_{J \rightarrow \infty} e(J) \rightarrow 0$.*

Proof: It follows from Lemma 1 and the convergence theorem of CSSCA in [26] that, starting from a feasible initial point, every limiting point $(\mathbf{x}^*, \boldsymbol{\lambda}^*)$ generated by Algorithm 1 is a stationary point $\mathbf{x}^*, \boldsymbol{\lambda}^*$ of the long-term sub-problem \mathcal{P}_L^J almost surely, providing that the initial step size γ^0 is sufficiently small, and the Slater condition is satisfied for $\mathbf{x}^*, \boldsymbol{\lambda}^*$. Then, it follows from the relaxed primal-dual decomposition method in Theorem 2 that the solution $(\mathbf{x}^*, \Theta^* = \{\mathbf{y}^J(\mathbf{x}^*, \boldsymbol{\lambda}^*, \boldsymbol{\xi}), \forall \boldsymbol{\xi}\})$ found by the PDD-SSCA (Algorithm 1) is a KKT solution of the original problem \mathcal{P} , up to certain error $e(J)$ that diminishes to zero as $J \rightarrow \infty$. ■

Note that due to the stochastic nature of the problem/algorithm, we need to assume that the step size is sufficiently small to make it easier to handle the randomness caused by the random state for tractable convergence analysis and rigorous convergence proof. However, choosing a small γ^0 is usually not mandatory for the practical convergence of Algorithm 1 as it is a sufficient not a necessary condition. In the simulations, we find that the algorithm can still converge even when the initial step size γ^0 is not small. In fact, in practice, we may prefer to choose a not very small γ^0 to achieve a faster initial convergence speed. Finally, we discuss the convergence behavior of Algorithm 1 with an infeasible initial point. Again, starting from a feasible initial point is just a sufficient not a necessary condition. Due to the feasible update in (19), Algorithm 1 still converges to a KKT solution of Problem (1) with high probability, even when the initial point is infeasible [26].

V. DEEP UNROLLING BASED IMPLEMENTATION

A. Motivation of Deep Unrolling based Implementation

In the long-term sub-algorithm, we need to calculate the gradient of $\mathbf{y}^J(\mathbf{x}, \boldsymbol{\lambda}, \boldsymbol{\xi})$ w.r.t. the long-term variables \mathbf{x} and $\boldsymbol{\lambda}$: $\partial_{\mathbf{x}} \mathbf{y}^J(\mathbf{x}, \boldsymbol{\lambda}, \boldsymbol{\xi})$ and $\partial_{\boldsymbol{\lambda}} \mathbf{y}^J(\mathbf{x}, \boldsymbol{\lambda}, \boldsymbol{\xi})$, where $\mathbf{y}^J(\mathbf{x}, \boldsymbol{\lambda}, \boldsymbol{\xi})$ is obtained by running the short-term sub-algorithm for J iterations. Since $\mathbf{y}^J(\mathbf{x}, \boldsymbol{\lambda}, \boldsymbol{\xi})$ involves an iterative algorithm, it is usually not easy to calculate its gradient in closed-form. One possible solution is to treat the iterative short-term sub-algorithm as a black-box, and learn the mapping $\mathbf{y}^J(\mathbf{x}, \boldsymbol{\lambda}, \boldsymbol{\xi})$ between the input and the output by employing the DNN. Once we obtain a DNN representation of the mapping $\mathbf{y}^J(\mathbf{x}, \boldsymbol{\lambda}, \boldsymbol{\xi})$, we can calculate the gradients $\partial_{\mathbf{x}} \mathbf{y}^J(\mathbf{x}, \boldsymbol{\lambda}, \boldsymbol{\xi})$ and $\partial_{\boldsymbol{\lambda}} \mathbf{y}^J(\mathbf{x}, \boldsymbol{\lambda}, \boldsymbol{\xi})$ using the well-known back propagation (BP) approach. Some representative studies of such a solution can be found in [15]–[17] for different applications. For example, in [15], the authors applied the multi-layer perceptron (MLP) and convo-

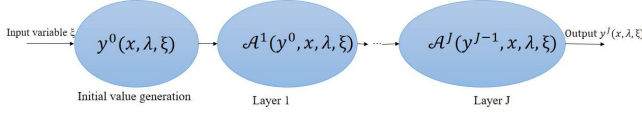


Figure 2: The NN representation of the short-term sub-algorithm.

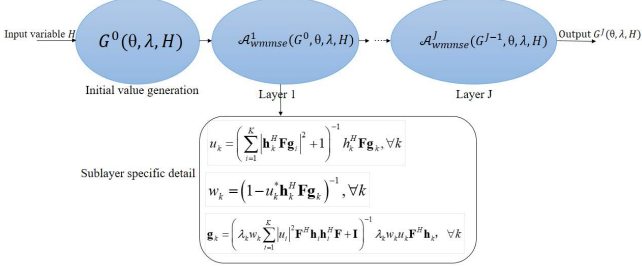


Figure 3: The NN representation of the WMMSE short-term sub-algorithm.

lutional neural network (CNN) to approximate the iterative WMMSE algorithm used in Example 2.

However, the black-box based DNNs suffer from poor interpretability and generalization ability, and have no performance guarantee. Moreover, the black-box based DNN often has a large number of parameters and requires a lot of training samples, which incurs high training complexity and memory overhead. To overcome such drawbacks, a number of works [30]–[32] have proposed to unfold the iterations into a layer-wise structure analogous to a NN based on the existing iterative algorithms. This method is referred to as deep unrolling/unfolding and has a wide range of applications in communications and signal processing. Compared to the black-box based DNN, the deep unrolling based NN tends to have better interpretability and generalization ability, as well as much lower training complexity and memory overhead. Therefore, in this paper, we propose to use the deep unrolling method to obtain a NN representation of the mapping $\mathbf{y}^J(\mathbf{x}, \boldsymbol{\lambda}, \boldsymbol{\xi})$ (or equivalently, the short-term sub-algorithm).

B. Deep Unrolling of the Short-term Sub-Algorithm

We can apply the deep unrolling technique to obtain a NN representation of the short-term sub-algorithm, where the input is $\boldsymbol{\xi}$, the output is $\mathbf{y}^J(\mathbf{x}, \boldsymbol{\lambda}, \boldsymbol{\xi})$, the 0-th layer is used to generate the initial value $\mathbf{y}^0(\mathbf{x}, \boldsymbol{\lambda}, \boldsymbol{\xi})$, and the j -th layer for $j = 1, \dots, J$ is simply given by $\mathcal{A}^j(\mathbf{y}^{j-1}(\mathbf{x}, \boldsymbol{\lambda}, \boldsymbol{\xi}), \mathbf{x}, \boldsymbol{\lambda}, \boldsymbol{\xi})$, as illustrated in Fig. 2.

To be more specific, in Fig. 3, we illustrate the NN representation of the WMMSE short-term sub-algorithm for application example 2. In this case, the input is the channel state \mathbf{H} , the output is the digital precoder $\mathbf{G}^J(\boldsymbol{\theta}, \boldsymbol{\lambda}, \mathbf{H})$, the 0-th layer is used to generate the initial value $\mathbf{G}^0(\boldsymbol{\theta}, \boldsymbol{\lambda}, \mathbf{H})$, and the j -th layer $\mathcal{A}^j(\mathbf{G}^{j-1}, \boldsymbol{\theta}, \boldsymbol{\lambda}, \mathbf{H})$ is given by the update equations in (29) to (31), where \mathbf{G}^{j-1} is an abbreviation for $\mathbf{G}^{j-1}(\boldsymbol{\theta}, \boldsymbol{\lambda}, \mathbf{H})$.

With the NN representation of the short-term sub-algorithm, we can use BP to calculate the gradients

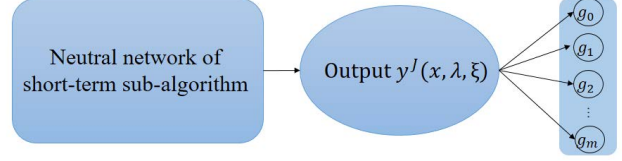


Figure 4: NN to calculate the gradients of g_i 's.

$\partial_{\mathbf{x}} \mathbf{y}^J(\mathbf{x}, \boldsymbol{\lambda}, \boldsymbol{\xi})$ and $\partial_{\boldsymbol{\lambda}} \mathbf{y}^J(\mathbf{x}, \boldsymbol{\lambda}, \boldsymbol{\xi})$ for the optimization of long-term variables. In fact, we can directly use BP to calculate $\partial_{\mathbf{x}} \mathbf{y}^J(\mathbf{x}, \boldsymbol{\lambda}, \boldsymbol{\xi}) \partial_{\mathbf{y}} g_i(\mathbf{x}, \mathbf{y}^J(\mathbf{x}, \boldsymbol{\lambda}, \boldsymbol{\xi}), \boldsymbol{\xi}), \forall i$ and $\partial_{\boldsymbol{\lambda}} \mathbf{y}^J(\mathbf{x}, \boldsymbol{\lambda}, \boldsymbol{\xi}) \partial_{\mathbf{y}} g_i(\mathbf{x}, \mathbf{y}^J(\mathbf{x}, \boldsymbol{\lambda}, \boldsymbol{\xi}), \boldsymbol{\xi}), \forall i$ at $(\mathbf{x}, \boldsymbol{\lambda}) = (\mathbf{x}^t, \boldsymbol{\lambda}^t)$ by adding an additional layer to implement the function $g_i(\mathbf{x}^t, \mathbf{y}^J(\mathbf{x}, \boldsymbol{\lambda}, \boldsymbol{\xi}), \boldsymbol{\xi}), \forall i$ on top of the NN representation of the short-term sub-algorithm, as shown in Fig. 4. Note that the calculations for different i using BP share the same calculations over the NN of the short-term sub-algorithm. With $\partial_{\mathbf{x}} \mathbf{y}^J(\mathbf{x}, \boldsymbol{\lambda}, \boldsymbol{\xi}) \partial_{\mathbf{y}} g_i(\mathbf{x}, \mathbf{y}^J(\mathbf{x}, \boldsymbol{\lambda}, \boldsymbol{\xi}), \boldsymbol{\xi}), \forall i$ and $\partial_{\boldsymbol{\lambda}} \mathbf{y}^J(\mathbf{x}, \boldsymbol{\lambda}, \boldsymbol{\xi}) \partial_{\mathbf{y}} g_i(\mathbf{x}, \mathbf{y}^J(\mathbf{x}, \boldsymbol{\lambda}, \boldsymbol{\xi}), \boldsymbol{\xi}), \forall i$ calculated by BP, the long-term variables $\mathbf{x}, \boldsymbol{\lambda}$ can be optimized based on the statistics of the random state $\boldsymbol{\xi}$, or a data set containing a large number of N state samples $\boldsymbol{\xi}^t, t = 1, \dots, N$, where the state samples can also be observed in an online manner. Once the optimized long-term variables $\mathbf{x}, \boldsymbol{\lambda}$ is obtained, the short-term variables $\mathbf{y}^J(\mathbf{x}, \boldsymbol{\lambda}, \boldsymbol{\xi})$ for each random state $\boldsymbol{\xi}$ can be calculated in an online manner using the NN representation.

C. Discussions on Possible Extensions

In this paper, we focus on the case when the short sub-algorithm is designed based on the optimization theory and is then unrolled without any modifications to facilitate the calculation of gradient. In practical implementation, we may add some additional layers/parameters to the NN unrolled from a short-term sub-algorithm (such as the GP, MM or WMMSE), and represent the mapping $\mathbf{y}^J(\mathbf{x}, \boldsymbol{\lambda}, \boldsymbol{\xi})$ using a more general NN as $\mathbf{y}^J(\mathbf{x}, \boldsymbol{\lambda}, \boldsymbol{\xi}) = \phi(\mathbf{x}, \boldsymbol{\lambda}, \boldsymbol{\xi}; \boldsymbol{\theta})$, where the vector $\boldsymbol{\theta}$ contains the additional parameters. These additional layers/parameters can be optimized to potentially speed up the convergence speed or even improve the performance. For example, for a GP short-term sub-algorithm, we may change the update equation in (22) to

$$\mathcal{A}^j(\mathbf{y}^{j-1}) = \mathbb{P}_{\mathbf{y}(\mathbf{x}, \boldsymbol{\lambda}, \boldsymbol{\xi})} [\mathbf{y}^{j-1} - \boldsymbol{\alpha}_j \circ \partial_{\mathbf{y}} g_s(\mathbf{x}, \boldsymbol{\lambda}, \mathbf{y}^{j-1}, \boldsymbol{\xi})],$$

where the scalar step size α_j in the original GP update equation (22) is expanded to a vector step size $\boldsymbol{\alpha}_j$, and \circ denotes the Hadamard product. Since the vector step size $\boldsymbol{\alpha}_j$ includes the scalar step size α_j as a special case, we may optimize the vector step sizes $\{\boldsymbol{\alpha}_j, j = 1, \dots, J\}$ to achieve a better performance.

After introducing the additional layers/parameters, both the parameter $\boldsymbol{\theta}$ and the long-term variables $\mathbf{x}, \boldsymbol{\lambda}$ can be optimized by solving the following modified long-term problem:

$$\hat{\mathcal{P}}_L : \min_{\mathbf{x}, \boldsymbol{\lambda}, \boldsymbol{\theta}} \hat{f}_0(\mathbf{x}, \boldsymbol{\lambda}, \boldsymbol{\theta}) \triangleq \mathbb{E}[g_0(\mathbf{x}, \phi(\mathbf{x}, \boldsymbol{\lambda}, \boldsymbol{\xi}; \boldsymbol{\theta}), \boldsymbol{\xi})], \quad (33)$$

$$\text{s.t. } \hat{f}_i(\mathbf{x}, \boldsymbol{\lambda}, \boldsymbol{\theta}) \triangleq \mathbb{E}[g_i(\mathbf{x}, \phi(\mathbf{x}, \boldsymbol{\lambda}, \boldsymbol{\xi}; \boldsymbol{\theta}), \boldsymbol{\xi})] \leq 0, \forall i.$$

Note that since the original short-term sub-algorithm $\mathbf{y}^J(\mathbf{x}, \boldsymbol{\lambda}, \boldsymbol{\xi})$ is a special case of the NN $\phi(\mathbf{x}, \boldsymbol{\lambda}, \boldsymbol{\xi}; \boldsymbol{\theta})$, it is expected that a better objective value can be potentially achieved by solving $\hat{\mathcal{P}}_L$ due to the extra freedom introduced by the additional parameters $\boldsymbol{\theta}$. Problem $\hat{\mathcal{P}}_L$ can be solved using the same CSSCA method as in Algorithm 1, with $\boldsymbol{\theta}$ as an additional long-term variable. Once the optimized long-term variables $\mathbf{x}, \boldsymbol{\lambda}, \boldsymbol{\theta}$ is obtained, the short-term variables $\mathbf{y}^J(\mathbf{x}, \boldsymbol{\lambda}, \boldsymbol{\xi}) = \phi(\mathbf{x}, \boldsymbol{\lambda}, \boldsymbol{\xi}; \boldsymbol{\theta})$ for each random state $\boldsymbol{\xi}$ can be calculated in an online manner using the NN representation. Therefore, we may view the Algorithm 1 as an unsupervised learning algorithm for the additional parameters $\boldsymbol{\theta}$. It is also possible to pre-train $\boldsymbol{\theta}$ using a supervised learning algorithm. Then we may use the pre-trained $\boldsymbol{\theta}$ as an initial point for the Algorithm 1. The pre-training helps to speed up the convergence speed or even improve the performance.

Finally, we give an example to briefly illustrate how to unfold the WMMSE short-term sub-algorithm in Example 2, based on the deep-unfolding framework proposed in [32], where a general form of iterative algorithm induced deep unfolding neural network (IAIDNN) is developed in matrix form to better solve optimization problems in communication systems. Specifically, the iterative WMMSE algorithm is unfolded into a layer-wise structure with a series of matrix multiplication and non-linear operations, as illustrated in Fig. 2 in [32]. Compared to the original WMMSE iterations, there are two major modifications. First, the element-wise non-linear function and the first-order Taylor expansion structure of the inverse matrix is applied to approximate the matrix inversion operation in the WMMSE algorithm. Second, trainable parameters $\boldsymbol{\theta}$ are introduced in the non-linear function and the first-order Taylor expansion structure of the inverse matrix, aiming at compensating the performance loss caused by the approximation of matrix inversion. Such modifications help to greatly speed up the convergence speed and reduce the complexity of each iteration (layer) with little performance loss. Then, the training process can be divided into the following two stages. In the supervised learning stage, the expected distance between the output of the IAIDNN $\mathbf{G}(\mathbf{x}, \boldsymbol{\lambda}, \boldsymbol{\xi})$ and the labels produced by the iterative WMMSE algorithm $\mathbf{G}^*(\mathbf{x}, \boldsymbol{\lambda}, \boldsymbol{\xi})$ under different long-term variables $\mathbf{x}, \boldsymbol{\lambda}$ and channel realizations $\boldsymbol{\xi}$ is used as the loss function to pre-train $\boldsymbol{\theta}$, with learning rate $\max(0.1n^{-0.5}, 10^{-4})$ and training batch size 100, where n denotes the training iteration number. Please refer to [32] for more details. After applying the supervised learning, Algorithm 1 can be used to optimize/train both the long-term variables $\mathbf{x}, \boldsymbol{\lambda}$ and the parameter $\boldsymbol{\theta}$ in an unsupervised way.

VI. APPLICATIONS

In this section, we shall apply the proposed PDD-SSCA to solve the two applications described in Section II-B. In both applications, we assume that the channel statistics is known at the optimizer, and the *coherence time of the channel statistics* (within which the channel statistics is assumed to be constant) consists of $T_c = 1000$ channel realizations. The optimization algorithms first calculate the optimal long-term variables at the

	Example 1	Example 2
Batch Size B	20	20
Step size ρ^t	$10/(10+n)^{0.9}$	$10/(10+n)^{0.9}$
Step size γ^t	$15/(15+n)$	$15/(15+n)$
Number of Layers J	N/A	5

Table I: Parameters of the proposed PDD-SSCA algorithm used in the simulations.

beginning of the channel statistics coherence time according to the known channel statistics, and then solve the short-term subproblem to obtain the short-term variables for each channel realization. The simulation results are also obtained by averaging over $T_c = 1000$ channel realizations. The key algorithm parameters used in the simulations are shown in Table I.

A. Cognitive Multiple Access Channels

In this example, the sample objective and constraint functions for a fixed state \mathbf{a}, \mathbf{b} are given by

$$\begin{aligned} g_0(\boldsymbol{\lambda}, \Upsilon, \mathbf{a}, \mathbf{b}) &= \log \left(1 + \sum_{i=1}^N \frac{1}{N} \left(\frac{a_i}{b_i \Upsilon + \lambda_i} - 1 \right)^+ \right), \\ g_i(\boldsymbol{\lambda}, \Upsilon, \mathbf{a}, \mathbf{b}) &= \frac{1}{Na_i} \left(\frac{a_i}{b_i \Upsilon + \lambda_i} - 1 \right)^+ - P_i, \\ g_{N+1}(\boldsymbol{\lambda}, \Upsilon, \mathbf{a}, \mathbf{b}) &= \sum_{i=1}^N \frac{b_i}{Na_i} \left(\frac{a_i}{b_i \Upsilon + \lambda_i} - 1 \right)^+ - \Gamma, \end{aligned} \quad (34)$$

for $i = 1, \dots, N$, where $g_i(\boldsymbol{\lambda}, \Upsilon, \mathbf{a}, \mathbf{b})$ is an abbreviation for $g_i(\mathbf{p}^*(\boldsymbol{\lambda}, \Upsilon, \mathbf{a}, \mathbf{b}), \mathbf{a}, \mathbf{b})$, and $\mathbf{p}^*(\boldsymbol{\lambda}, \Upsilon, \mathbf{a}, \mathbf{b})$ is the optimal short-term power allocation in (25). To construct the surrogate function, we first calculate the gradients $\nabla_{\boldsymbol{\lambda}} g_i(\boldsymbol{\lambda}, \Upsilon, \mathbf{a}, \mathbf{b})$ and $\nabla_{\Upsilon} g_i(\boldsymbol{\lambda}, \Upsilon, \mathbf{a}, \mathbf{b})$ for $i = 0, 1, \dots, N+1$. The calculation is straightforward from (34) and the details are omitted for conciseness. Note that strictly speaking, g_i is non-differentiable when $\frac{a_i}{b_i \Upsilon + \lambda_i} - 1 = 0$. However, since the probability of $\frac{a_i}{b_i \Upsilon + \lambda_i} - 1 = 0$ is very small (zero for continuous state distribution), we can safely ignore this point. With the gradients of g_i 's, we can construct quadratic surrogate functions as

$$\begin{aligned} \bar{f}_i^t(\boldsymbol{\lambda}, \Upsilon) &= f_i^t + (\mathbf{f}_{\boldsymbol{\lambda}, i}^t)^T (\boldsymbol{\lambda} - \boldsymbol{\lambda}^t) + (\mathbf{f}_{\Upsilon, i}^t)^T (\Upsilon - \Upsilon^t) \\ &\quad + \tau_i \left(\|\boldsymbol{\lambda} - \boldsymbol{\lambda}^t\|^2 + (\Upsilon - \Upsilon^t)^2 \right), \end{aligned} \quad (35)$$

p'pwhere $\mathbf{f}_{\boldsymbol{\lambda}, i}^t$ and $\mathbf{f}_{\Upsilon, i}^t$ can be calculated recursively as

$$\begin{aligned} \mathbf{f}_{\Upsilon, i}^t &= (1 - \rho^t) \mathbf{f}_{\Upsilon, i}^{t-1} + \rho^t \frac{1}{B} \sum_{j=1}^B \nabla_{\Upsilon} g_i(\boldsymbol{\lambda}^t, \Upsilon^t, \mathbf{a}_j^t, \mathbf{b}_j^t), \\ \mathbf{f}_{\boldsymbol{\lambda}, i}^t &= (1 - \rho^t) \mathbf{f}_{\boldsymbol{\lambda}, i}^{t-1} + \rho^t \frac{1}{B} \sum_{j=1}^B \nabla_{\boldsymbol{\lambda}} g_i(\boldsymbol{\lambda}^t, \Upsilon^t, \mathbf{a}_j^t, \mathbf{b}_j^t). \end{aligned} \quad (36)$$

Note that the quadratic surrogate function in (35) is a special case of the structured surrogate function in (16) when $g_i^c(\mathbf{x}, \mathbf{y}, \boldsymbol{\xi})$ is set to be 0. In this case, both the objective update (18) and the feasible update (19) are simple quadratic optimization problems, which can be solved efficiently using the existing optimization solvers such as CVX [33].

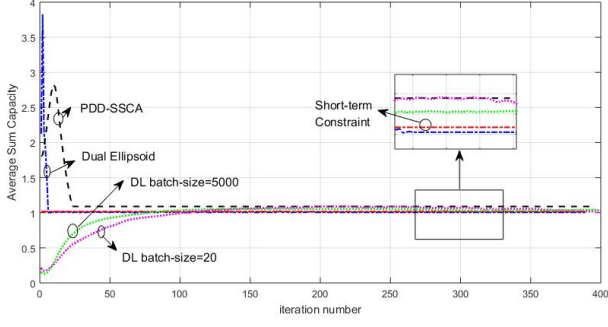


Figure 5: Average sum capacity versus iteration number.

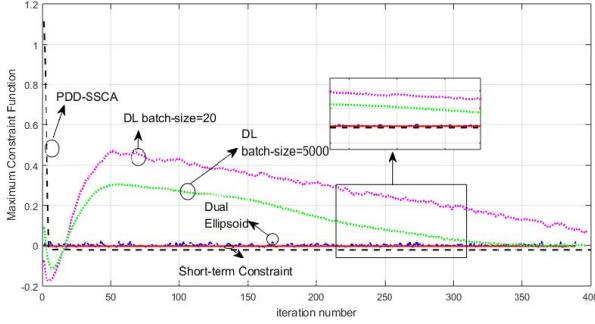


Figure 6: Maximum constraint function versus iteration number.

We compare the proposed PDD-SSCA with the following baseline algorithms.

- **Baseline 1 (DL):** This is the DL algorithm in [18].
- **Baseline 2 (Dual Ellipsoid):** This is the dual decomposition algorithm in [19]. The dual problem is solved using the Ellipsoid method [34]. Note that the dual decomposition is applicable to Example 1 because this problem is convex. In each iteration of the Ellipsoid method, the expectation $\mathbb{E}[g_i(\lambda, \Upsilon, \mathbf{a}, \mathbf{b})]$, $\forall i$ is required to calculate the subgradient, which is obtained by sample averaging over $T_c = 1000$ channel realizations.
- **Baseline 3 (Short-term Constraint):** Example Problem 1 is optimally solved with the short-term constraints $p_i(\mathbf{a}, \mathbf{b}) \leq P_i$ and $\sum_{i=1}^N b_i p_i(\mathbf{a}, \mathbf{b}) \leq \Gamma$, instead of $\mathbb{E}[p_i(\mathbf{a}, \mathbf{b})] \leq P_i$ and $\mathbb{E}[\sum_{i=1}^N b_i p_i(\mathbf{a}, \mathbf{b})] \leq \Gamma$.

Following the same simulation configuration as in [18], we set $N = 2$, $\Gamma = 0.5$, $P_i = P = 5$ dB, $\forall i$. In Figs. 5 and 6, we plot the objective function (average sum capacity) and maximum constraint function versus the iteration number,

	Complexity order per iteration	Mem. cost
Proposed	$O(I_1(N \log N + B_1 N) + T_c N)$	$O(B_1 N)$
DL	$O(I_2 B_2 100 N^2 L + T_c N)$	$O(B_2 N + 100 N^2 L)$
Dual Ellipsoid	$O(I_3(N^2 + T_c N) + T_c N)$	$O(N T_c)$
Baseline 3	$O(T_c N^2)$	$O(N)$

Table II: Comparison of the complexity order and memory cost for different algorithms in Example 1.

respectively. The per-iteration computation complexity and memory cost are compared in Table II, where the $B_i, i = 1, 2$ and $I_i, i = 1, 2, 3$ account for the mini-batch size and the number of iterations for optimizing the long-term variables, respectively. The complexity of calculating the estimated long-term gradient is $O(B_1 N)$ for mini-batch size B_1 . The complexity of solving the objective update problem in (18) or the feasibility update problem in (19) using the interior-point method is given by $O(N(\log(N)))^2$. Moreover, the complexity of calculating the optimal short-term solution is $O(N)$ per channel realization. Therefore, the per-iteration complexity order of the proposed algorithm is as given in Table II. The memory cost is proportional to the amount of parameters to be optimized plus the product of the batch size and the dimension of the state variable, i.e., $O(B_1 N)$ Bytes. The complexity order and memory cost of the baseline algorithms can be analyzed similarly. PDD-SSCA converges to the optimal average sum capacity with all average transmit power constraints and interference threshold constraint satisfied with high accuracy. For the same batch size 20, the number of iterations required to achieve a good convergence accuracy in the proposed PDD-SSCA is much less than that in the DL (25 versus more than 400). Moreover, the complexity/memory cost of the PDD-SSCA is also much less than that of the DL since it exploits the structure of the problem and has much less parameters to be optimized (3 versus 2080). When the batch size of the DL is increased to 5000, the required number of iterations of DL can be reduced (but still much larger than 25), at the cost of dramatically increasing the complexity and memory cost. Both the convergence speed and performance of the PDD-SSCA are similar to that of the Dual Ellipsoid method. However, the complexity and memory cost of the PDD-SSCA are much lower. Therefore, the proposed PDD-SSCA is much more efficient than the DL and Dual Ellipsoid methods. Finally, the complexity/memory cost of the PDD-SSCA is similar to/slightly higher than the ‘‘Short-term Constraint’’ baseline, but the performance is much better.

B. Power Minimization for Two-timescale Hybrid Beamforming

In this example, the short-term WMMSE algorithm can be implemented using a simple NN as shown in Fig. 3. Moreover, the gradients of the sample objective and constraint functions $\nabla_{\theta} g_i(\theta, \mathbf{G}^J(\theta, \lambda, \mathbf{H}), \mathbf{H})$ and $\nabla_{\lambda} g_i(\theta, \mathbf{G}^J(\theta, \lambda, \mathbf{H}), \mathbf{H})$ for a fixed state \mathbf{H} can be calculated using the BP method based on the NN in Fig. 4. Then, we can construct quadratic surrogate functions as

$$\begin{aligned} \bar{f}_i^t(\theta, \lambda) &= f_i^t + (\mathbf{f}_{\theta,i}^t)^T (\theta - \theta^t) + (\mathbf{f}_{\lambda,i}^t)^T (\lambda - \lambda^t) \\ &\quad + \tau_i \left(\|\theta - \theta^t\|^2 + \|\lambda - \lambda^t\|^2 \right), \end{aligned} \quad (37)$$

²This is because the objective/feasibility update problem is a convex quadratic programming problem with a diagonal Hessian matrix.

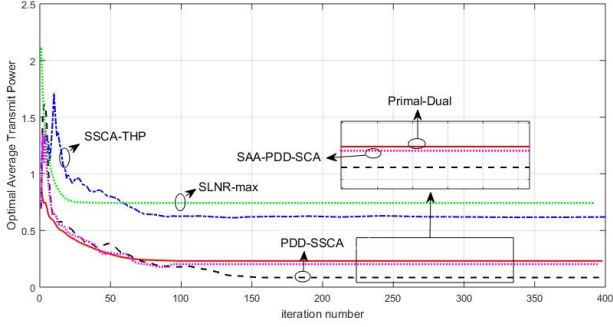


Figure 7: Average transmit power versus iteration number.

where $\mathbf{f}_{\theta,i}^t$ and $\mathbf{f}_{\lambda,i}^t$ can be calculated recursively as

$$\begin{aligned} \mathbf{f}_{\theta,i}^t &= (1 - \rho^t) \mathbf{f}_{\theta,i}^{t-1} + \rho^t \frac{1}{B} \sum_{j=1}^B \nabla_{\theta} g_i(\theta^t, \lambda^t, \mathbf{H}_j^t), \\ \mathbf{f}_{\lambda,i}^t &= (1 - \rho^t) \mathbf{f}_{\lambda,i}^{t-1} + \rho^t \frac{1}{B} \sum_{j=1}^B \nabla_{\lambda} g_i(\theta^t, \lambda^t, \mathbf{H}_j^t), \end{aligned} \quad (38)$$

where $g_i(\theta^t, \lambda^t, \mathbf{H}_j^t)$ is an abbreviation for $g_i(\theta^t, \mathbf{G}^J(\theta^t, \lambda^t, \mathbf{H}_j^t), \mathbf{H}_j^t)$. Again, both the objective update (18) and the feasible update (19) are simple quadratic optimization problems, which can be solved efficiently.

We compare the proposed PDD-SSCA with the following baseline algorithms.

- **Baseline 1 (SSCA-THP):** The SSCA-THP in [35] is a single-stage optimization algorithm which only optimizes the RF precoder θ with the baseband precoder fixed as the regularized zero-forcing (RZF) precoder [36].
- **Baseline 2 (Prima-Dual):** This is a primal-dual method based algorithm, in which the primal-dual method in [18] is employed to solve the long-term problem in (14) and the rest is similar to the proposed algorithm.
- **Baseline 3 (SAA-PDD-SSCA):** Sample average approximation (SAA) is a common method to solve a stochastic optimization problem [37], at the cost of high computation and memory overhead. After applying the SAA on the constraint functions using 200 channel samples, the problem becomes a deterministic optimization problem with coupled non-convex constraints. We apply the proposed primal-dual decomposition to decompose this deterministic problem into one master problem (optimization of RF precoding and long-term Lagrange multipliers) and 200 subproblems (optimization of digital precoding). Then in each iteration, the master problem is solved using the deterministic SCA method in [28] and the digital precoding optimization subproblems are solved using the WMMSE method.
- **Baseline 4 (SLNR-max):** This is the SLNR-max algorithm in [22]. The RF precoder is optimized by maximizing the signal-to-leakage plus noise ratio (SLNR) [22]. Then the digital precoder for each channel realization is optimized using the WMMSE method by solving a power minimization problem subject to the rate constraint.

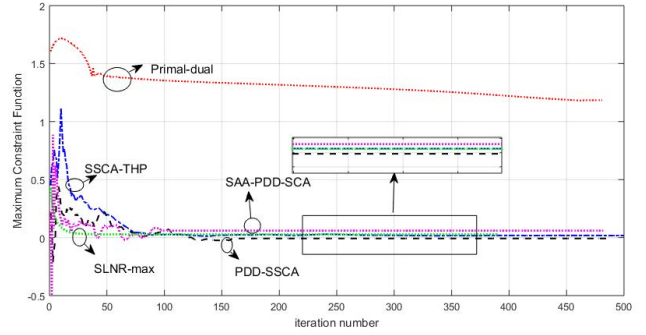


Figure 8: Maximum constraint function versus iteration number.

In the simulations, we adopt the same geometry-based channel model as in [22], [35]. There are $M = 64$ antennas and $S = 4$ RF chains at the BS, serving $K = 4$ users. In Figs. 7 and 8, we plot the objective function (average transmit power) and maximum constraint function (target average rate minus achieved average rate) versus the iteration, respectively. The per-iteration computation complexity and memory cost are compared in Table III, where the B_i and I_i account for the mini-batch size and the number of iterations for optimizing the long-term variables, I_W is the number iterations of WMMSE algorithm. We set $B_1 = 20$ and $B_2 = 200$ in the simulations. The complexity order of the short-term WMMSE algorithm is given by $O(I_W S^3)$. The complexity of calculating the estimated long-term gradient is $O(B_1 I_W S^3)$ for mini-batch size B_1 . The complexity of solving the objective/feasibility update problem using the interior-point method is given by $O(M S \log(K))$. Moreover, the complexity of calculating the optimal short-term solution is $O(I_W S^3)$ per channel realization. Therefore, the per-iteration complexity order of the proposed algorithm is as given in Table III. The memory cost is proportional to the amount of parameters to be optimized plus the product of the batch size and the dimension of the state variable, i.e., $O(MS + B_1 MK)$ Bytes. The complexity order and memory cost of the baseline algorithms can be analyzed similarly. The number of iteration required to achieve a good convergence accuracy in the proposed PDD-SSCA is similar to that in the SSCA-THP. However, the PDD-SSCA converges to a much lower average transmit power with all target average rates satisfied with high accuracy. The PDD-SSCA can achieve a large performance gain over the SSCA-THP. On the other hand, the primal-dual method based algorithm cannot converge to a feasible solution that satisfies all the average rate constraints, due to the highly non-convex nature of the constraints. The convergence speed of the PDD-SSCA is similar to that of the SAA-PDD-SSCA method. However, the performance of the PDD-SSCA is better because using $B_2 = 200$ samples is not sufficient to obtain a good sample average approximation, and the complexity/memory cost of the PDD-SSCA is also much lower. Finally, the complexity/memory cost of the PDD-SSCA is lower than the SLNR-max baseline, and the performance is much better.

	Complexity order per iteration	Memory cost
Proposed	$O(I_1(MS \log K + B_1 I_W S^3) + T_c I_W S^3)$	$O(MS + B_1 MK)$
SSCA-THP	$O(I_2(MS \log(K) + B_1 S^3) + T_c S^3)$	$O(MS + B_1 MK)$
Prima-Dual	$O(I_3(MS + B_1 I_W S^3) + T_c I_W S^3)$	$O(MS + B_1 MK)$
SAA-PDD-SCA	$O(I_4(MS \log K + B_2 I_W S^3) + T_c I_W S^3)$	$O(MS + B_2 MK)$
SLNR-max	$O(I_5 M^3 + T_c I_W S^3)$	$O(KM^2)$

Table III: Comparison of the complexity order and memory cost for different algorithms in Example 2.

C. Conclusions

We propose a PDD-SSCA algorithmic framework to solve a class of two-stage stochastic optimization problems, in which the long-term and short-term variables are tightly coupled in non-convex stochastic constraints. The PDD-SSCA is designed based on a novel two-stage primal-dual decomposition method established in this paper, which shows that the tightly coupled two-stage problem can be decomposed into a long-term problem and a family of short-term subproblems. At each iteration, PDD-SSCA first runs a short-term sub-algorithm to find stationary points of the short-term subproblems associated with a mini-batch of the state samples. Then it constructs a convex surrogate for the long-term problem based on the deep unrolling of the short-term sub-algorithm and the back propagation method. Finally, the optimal solution of the convex surrogate problem is solved to generate the next iterate. We show that under some technical conditions, PDD-SSCA converges to a KKT solution of the original two-stage problem almost surely. The effectiveness of the proposed PDD-SSCA method is verified using two important application examples.

APPENDIX

1) *Proof of Theorem 1* : Using the condition $\delta_i \in (0, G_i^{\max}(\mathbf{x}^\circ) - G_i^{\min}(\mathbf{x}^\circ))$, $\forall i$ and following similar analysis as that in the proof of Proposition 2 of [18], it can be shown that for fixed \mathbf{x}° , Problem \mathcal{P} fulfils the time-sharing condition [38] and the strong duality holds for \mathcal{P} with fixed \mathbf{x}° . Therefore, there must exist Lagrange multipliers λ° , such that Θ° is an optimal solution of the following problem:

$$\begin{aligned} \min_{\Theta} \mathbb{E}[g_0(\mathbf{x}^\circ, \mathbf{y}(\xi), \xi)] & \quad (39) \\ & + \sum_i \lambda_i^\circ \mathbb{E}[g_i(\mathbf{x}^\circ, \mathbf{y}(\xi), \xi)], \\ \text{s.t. } h_j(\mathbf{y}(\xi), \xi) \leq 0, j = 1, \dots, n, \forall \xi. \end{aligned}$$

Moreover,

$$\begin{aligned} \lambda_i^\circ \mathbb{E}[g_i(\mathbf{x}^\circ, \mathbf{y}^\circ(\xi), \xi)] &= 0, \forall i, \\ \mathbb{E}[g_i(\mathbf{x}^\circ, \mathbf{y}^\circ(\xi), \xi)] &\leq 0, \forall i. \end{aligned} \quad (40)$$

By definition, $\{\mathbf{y}^*(\mathbf{x}^\circ, \lambda^\circ, \xi), \forall \xi\}$ is also an optimal solution of (39) and satisfies

$$\begin{aligned} \lambda_i^\circ \mathbb{E}[g_i(\mathbf{x}^\circ, \mathbf{y}^*(\mathbf{x}^\circ, \lambda^\circ, \xi), \xi)] &= 0, \forall i, \\ \mathbb{E}[g_i(\mathbf{x}^\circ, \mathbf{y}^*(\mathbf{x}^\circ, \lambda^\circ, \xi), \xi)] &\leq 0, \forall i. \end{aligned} \quad (41)$$

From (40), (41) and the fact that both Θ° and $\{\mathbf{y}^*(\mathbf{x}^\circ, \lambda^\circ, \xi), \forall \xi\}$ are optimal solutions of (39), we have

$$\begin{aligned} f_0^*(\mathbf{x}^\circ, \lambda^\circ) &= \mathbb{E}[g_0(\mathbf{x}^\circ, \mathbf{y}^*(\mathbf{x}^\circ, \lambda^\circ, \xi), \xi)] \\ &= \mathbb{E}[g_0(\mathbf{x}^\circ, \mathbf{y}^\circ(\xi), \xi)] = f_0(\mathbf{x}^\circ, \Theta^\circ), \\ f_i^*(\mathbf{x}^\circ, \lambda^\circ) &= \mathbb{E}[g_i(\mathbf{x}^\circ, \mathbf{y}^*(\mathbf{x}^\circ, \lambda^\circ, \xi), \xi)] \leq 0, \forall i. \end{aligned}$$

Therefore, $\mathbf{x}^\circ, \lambda^\circ$ is a feasible solution of \mathcal{P}_L , and thus $f_0^*(\mathbf{x}^*, \lambda^*) \leq f_0^*(\mathbf{x}^\circ, \lambda^\circ) = f_0(\mathbf{x}^\circ, \Theta^\circ)$, from which it follows that $(\mathbf{x}^*, \lambda^*)$ is also the optimal solution of \mathcal{P} .

2) *Proof of Theorem 2* : We first prove a useful Lemma.

Lemma 2. Let $\mathcal{I}_A^S(\xi) = \{j : \nu_j(\mathbf{x}^*, \lambda^*, \xi) > 0\}$. We must have $\lim_{J \rightarrow \infty} \nabla_{\lambda} h_j(\mathbf{y}^{J*}, \xi) = \mathbf{0}, \forall j \in \mathcal{I}_A^S(\xi)$, where \mathbf{y}^{J*} is an abbreviation for $\mathbf{y}^J(\mathbf{x}^*, \lambda^*, \xi)$.

Proof: From the first KKT condition in (13), and the LIRC, it can be shown that $\nu_j(\mathbf{x}, \lambda, \xi)$ is differentiable w.r.t. λ and $\partial_{\lambda} \nu_j(\mathbf{x}^*, \lambda^*, \xi)$ is bounded. From the third KKT condition in (13), we have

$$\begin{aligned} \nabla_{\lambda} h_j(\mathbf{y}^{J*}, \xi) &= \frac{\partial_{\lambda} e_{3,j}^J(\mathbf{x}^*, \lambda^*, \xi)}{\nu_j(\mathbf{x}^*, \lambda^*, \xi)} \\ &\quad - \frac{e_{3,j}^J(\mathbf{x}^*, \lambda^*, \xi) \partial_{\lambda} \nu_j(\mathbf{x}^*, \lambda^*, \xi)}{\nu_j^2(\mathbf{x}^*, \lambda^*, \xi)}, \end{aligned} \quad (42)$$

$\forall j \in \mathcal{I}_A^S(\xi)$. Then Lemma 2 follows from (42) and the fact that $\nu_j(\mathbf{x}^*, \lambda^*, \xi) > 0, \forall j \in \mathcal{I}_A^S(\xi)$, $\partial_{\lambda} \nu_j(\mathbf{x}^*, \lambda^*, \xi)$ is bounded and $\lim_{J \rightarrow \infty} e_{3,j}^J(\mathbf{x}^*, \lambda^*, \xi) = 0$, $\lim_{J \rightarrow \infty} \partial_{\lambda} e_{3,j}^J(\mathbf{x}^*, \lambda^*, \xi) = \mathbf{0}$. ■

According to the chain rule,

$$\begin{aligned} \nabla_{\lambda} g_i(\mathbf{x}^*, \mathbf{y}^{J*}, \xi) &= \partial_{\lambda} \mathbf{y}^{J*} \partial_{\mathbf{y}} g_i(\mathbf{x}^*, \mathbf{y}^{J*}, \xi), \\ \nabla_{\lambda} h_j(\mathbf{y}^J(\mathbf{x}^*, \lambda^*, \xi), \xi) &= \partial_{\lambda} \mathbf{y}^{J*} \partial_{\mathbf{y}} h_j(\mathbf{y}^{J*}, \xi), \end{aligned}$$

where $\partial_{\lambda} \mathbf{y}^{J*} = \partial_{\lambda} \mathbf{y}^J(\mathbf{x}^*, \lambda^*, \xi) \in \mathbb{C}^{m \times n_y}$ are the derivative of the vector function $\mathbf{y}^J(\mathbf{x}, \lambda, \xi)$ to the vector λ at point \mathbf{x}^*, λ^* . Therefore, after multiplying both sides of the first KKT condition in (13) for $(\mathbf{x}, \lambda) = (\mathbf{x}^*, \lambda^*)$ with $\partial_{\lambda} \mathbf{y}^{J*}$ and taking expectation w.r.t. ξ , we have

$$\left\| \nabla_{\lambda} f_0^J(\mathbf{x}^*, \lambda^*) + \sum_i \lambda_i^* \nabla_{\lambda} f_i^J(\mathbf{x}^*, \lambda^*) \right\| = O(e(J)). \quad (43)$$

In (43), we have used Lemma 2. Combining (43) and the second KKT condition in (13), and, we have

$$\left\| \sum_{i \in \mathcal{I}_{IA}^L} \lambda_i^* \nabla_{\lambda} f_i^J(\mathbf{x}^*, \boldsymbol{\lambda}^*) - \sum_{i \in \mathcal{I}_A^L} (\tilde{\lambda}_i - \lambda_i^*) \nabla_{\lambda} f_i^J(\mathbf{x}^*, \boldsymbol{\lambda}^*) \right\| = O(e(J)) \quad (44)$$

where $\mathcal{I}_A^L = \{i : f_i^J(\mathbf{x}, \boldsymbol{\lambda}) = 0\}$ is the index set of the active long-term constraints, and $\mathcal{I}_{IA}^L = \{i : f_i^J(\mathbf{x}, \boldsymbol{\lambda}) < 0\}$ is the index set of the inactive long-term constraints. It follows from (44) and the LIRC that

$$\begin{aligned} \lambda_i^* &= O(e(J)), \forall i \in \mathcal{I}_{IA}^L, \\ \tilde{\lambda}_i - \lambda_i^* &= O(e(J)), \forall i \in \mathcal{I}_A^L, \end{aligned} \quad (45)$$

which indicates that the third KKT condition in (10) is satisfied up to error $O(e(J))$.

Similar to (43), it can be shown that

$$\begin{aligned} &\left\| \mathbb{E} [\partial_{\mathbf{x}} \mathbf{y}^{J*} \partial_{\mathbf{y}} g_0(\mathbf{x}^*, \mathbf{y}^{J*}, \boldsymbol{\xi})] \right. \\ &\left. + \sum_i \lambda_i^* \mathbb{E} [\partial_{\mathbf{x}} \mathbf{y}^{J*} \partial_{\mathbf{y}} g_i(\mathbf{x}^*, \mathbf{y}^{J*}, \boldsymbol{\xi})] \right\| = O(e(J)), \end{aligned} \quad (46)$$

where $\partial_{\mathbf{x}} \mathbf{y}^{J*} = \partial_{\mathbf{x}} \mathbf{y}^J(\mathbf{x}^*, \boldsymbol{\lambda}^*, \boldsymbol{\xi}) \in \mathbb{C}^{m \times n_y}$ is the derivative of the vector function $\mathbf{y}^J(\mathbf{x}, \boldsymbol{\lambda}, \boldsymbol{\xi})$ to the vector \mathbf{x} at point $\mathbf{x}^*, \boldsymbol{\lambda}^*$. Applying the chain rule to the first KKT condition in (15), we have

$$\begin{aligned} &\partial_{\mathbf{x}} f_0(\mathbf{x}^*, \Theta^*) + \sum_i \tilde{\lambda}_i \mathbb{E} [\partial_{\mathbf{x}} \mathbf{y}^{J*} \partial_{\mathbf{y}} g_i(\mathbf{x}^*, \mathbf{y}^{J*}, \boldsymbol{\xi})] \\ &+ \sum_i \tilde{\lambda}_i \partial_{\mathbf{x}} f_i(\mathbf{x}^*, \Theta^*) + \mathbb{E} [\partial_{\mathbf{x}} \mathbf{y}^{J*} \partial_{\mathbf{y}} g_0(\mathbf{x}^*, \mathbf{y}^{J*}, \boldsymbol{\xi})] = \mathbf{0}. \end{aligned} \quad (47)$$

Then it follows from (46), (45) and (47) that

$$\left\| \partial_{\mathbf{x}} f_0(\mathbf{x}^*, \Theta^*) + \sum_i \lambda_i^* \partial_{\mathbf{x}} f_i(\mathbf{x}^*, \Theta^*) \right\| = O(e(J)),$$

i.e., the second KKT condition in (10) is satisfied up to error $O(e(J))$.

Finally, it follows directly from (13) that the first KKT condition in (10) is satisfied up to error $O(e(J))$. This completes the proof.

3) *Proof of Lemma 1* : From Assumptions 1 and 2, $\partial_{\mathbf{x}}^T g_i^{\bar{e}}(\mathbf{x}^t, \mathbf{y}_j^t, \boldsymbol{\xi}_j^t)$, $\mathbf{f}_{x,i}^{t-1}$, $\mathbf{f}_{y,i}^t$ and $\mathbf{f}_{\lambda,i}^t$ are bounded. Therefore, Results 1) - 3) in Lemma 1 follow directly from the expression of the structured surrogate function in (16). Result 4) is true because $\lim_{t \rightarrow \infty} f_i^t - f_i^J(\mathbf{x}^t, \boldsymbol{\lambda}^t) = 0$, $\lim_{t \rightarrow \infty} \|\mathbf{f}_{x,i}^t + \mathbf{f}_{y,i}^t - \nabla_{\mathbf{x}} f_i^J(\mathbf{x}^t, \boldsymbol{\lambda}^t)\| = 0$ and $\lim_{t \rightarrow \infty} \|\mathbf{f}_{\lambda,i}^t - \nabla_{\lambda} f_i^J(\mathbf{x}^t, \boldsymbol{\lambda}^t)\| = 0$, which is a consequence of the chain rule and ([39], Lemma 1). The proof is similar to that of ([25], Lemma 1) and the details are omitted for conciseness. Finally, Result 5) is a consequence of Result 4).

REFERENCES

- [1] A. Liu, V. Lau, F. Zhuang, and J. Chen, "Two timescale joint beamforming and routing for multi-antenna D2D networks via stochastic cutting plane," *IEEE Trans. Signal Processing*, vol. 63, no. 18, pp. 4854–4865, Sept 2015.
- [2] A. Liu and V. K. N. Lau, "Two-stage constant-envelope precoding for low-cost massive MIMO systems," *IEEE Trans. Signal Processing*, vol. 64, no. 2, pp. 485–494, Jan. 2016.
- [3] —, "Two-timescale user-centric RRH clustering and precoding optimization for cloud RAN via local stochastic cutting plane," *IEEE Trans. Signal Processing*, vol. 66, no. 1, pp. 64–76, Jan 2018.
- [4] D. Hrabc, P. Popela, J. Roupec, J. Mazal, and P. Stodola, *Two-Stage Stochastic Programming for Transportation Network Design Problem*. Cham: Springer International Publishing, 2015, pp. 17–25.
- [5] J. R. Birge and F. Louveaux, *Introduction to Stochastic Programming*. Springer, 2011.
- [6] W. Lee, "Resource allocation for multi-channel underlay cognitive radio network based on deep neural network," *IEEE Communications Letters*, vol. 22, no. 9, pp. 1942–1945, Sept. 2018.
- [7] W. Lee, M. Kim, and D. Cho, "Transmit power control using deep neural network for underlay device-to-device communication," *IEEE Wireless Communications Letters*, vol. 8, no. 1, pp. 141–144, Feb. 2019.
- [8] Y. Sun, P. Babu, and D. P. Palomar, "Majorization-minimization algorithms in signal processing, communications, and machine learning," *IEEE Transactions on Signal Processing*, vol. 65, no. 3, pp. 794–816, Feb 2017.
- [9] G. Scutari, F. Facchinei, P. Song, D. P. Palomar, and J. S. Pang, "Decomposition by partial linearization: Parallel optimization of multi-agent systems," *IEEE Trans. Signal Processing*, vol. 62, no. 3, pp. 641–656, Feb 2014.
- [10] N. Komodakis and J. Pesquet, "Playing with duality: An overview of recent primal-dual approaches for solving large-scale optimization problems," *IEEE Signal Processing Magazine*, vol. 32, no. 6, pp. 31–54, 2015.
- [11] A. Tanikawa and H. Mukai, "A new technique for nonconvex primal-dual decomposition of a large-scale separable optimization problem," *IEEE Transactions on Automatic Control*, vol. 30, no. 2, pp. 133–143, 1985.
- [12] A. Berkelaar, J. A. S. Gromicho, R. Kouwenberg, and S. Zhang, "A primal-dual decomposition algorithm for multistage stochastic convex programming," *Mathematical Programming*, vol. 104, no. 1, pp. 153–177, 2005.
- [13] J. L. Hight and S. Sen, "Stochastic decomposition: An algorithm for two-stage linear programs with recourse," *Mathematics of Operations Research*, vol. 16, no. 3, pp. 650–669, 1991.
- [14] A. Liu, V. K. N. Lau, and M. Zhao, "Online successive convex approximation for two-stage stochastic nonconvex optimization," *IEEE Transactions on Signal Processing*, vol. 66, no. 22, pp. 5941–5955, Nov. 2018.
- [15] H. Sun, X. Chen, Q. Shi, M. Hong, X. Fu, and N. D. Sidiropoulos, "Learning to optimize: Training deep neural networks for interference management," *IEEE Transactions on Signal Processing*, vol. 66, no. 20, pp. 5438–5453, 2018.
- [16] W. Cui, K. Shen, and W. Yu, "Spatial deep learning for wireless scheduling," *IEEE Journal on Selected Areas in Communications*, vol. 37, no. 6, pp. 1248–1261, 2019.
- [17] B. Matthiesen, A. Zappone, K. L. Besser, E. A. Jorswieck, and M. Debbah, "A globally optimal energy-efficient power control framework and its efficient implementation in wireless interference networks," *IEEE Transactions on Signal Processing*, vol. 68, pp. 3887–3902, 2020.
- [18] H. Lee, S. H. Lee, and T. Q. S. Quek, "Deep learning for distributed optimization: Applications to wireless resource management," *IEEE Journal on Selected Areas in Communications*, vol. 37, no. 10, pp. 2251–2266, Oct. 2019.
- [19] R. Zhang, S. Cui, and Y. Liang, "On ergodic sum capacity of fading cognitive multiple-access and broadcast channels," *IEEE Transactions on Information Theory*, vol. 55, no. 11, pp. 5161–5178, Nov. 2009.
- [20] A. Liu and V. K. N. Lau, "Phase only RF precoding for massive MIMO systems with limited RF chains," *IEEE Trans. Signal Processing*, vol. 62, no. 17, pp. 4505–4515, Sept. 2014.
- [21] —, "Impact of CSI knowledge on the codebook-based hybrid beamforming in massive MIMO," *IEEE Transactions on Signal Processing*, vol. 64, no. 24, pp. 6545–6556, Dec 2016.
- [22] S. Park, J. Park, A. Yazdan, and R. W. Heath, "Exploiting spatial channel covariance for hybrid precoding in massive MIMO systems,"

- IEEE Trans. Signal Processing*, vol. 65, no. 14, pp. 3818–3832, July 2017.
- [23] X. Zhang, A. Molisch, and S.-Y. Kung, “Variable-phase-shift-based RF-baseband codesign for MIMO antenna selection,” *IEEE Trans. Signal Processing*, vol. 53, no. 11, pp. 4091–4103, Nov. 2005.
 - [24] J. Mairal, “Stochastic majorization-minimization algorithms for large-scale optimization,” in *Advances in Neural Information Processing Systems 26*, 2013, pp. 2283–2291.
 - [25] Y. Yang, G. Scutari, D. P. Palomar, and M. Pesavento, “A parallel decomposition method for nonconvex stochastic multi-agent optimization problems,” *IEEE Trans. Signal Processing*, vol. 64, no. 11, pp. 2949–2964, June 2016.
 - [26] A. Liu, V. K. N. Lau, and B. Kananian, “Stochastic successive convex approximation for non-convex constrained stochastic optimization,” *IEEE Transactions on Signal Processing*, vol. 67, no. 16, pp. 4189–4203, Aug. 2019.
 - [27] D. P. Bertsekas, *Nonlinear Programming*, 2nd ed. Belmont, MA: Athena Scientific, 1999.
 - [28] M. Razaviyayn, “Successive convex approximation: Analysis and applications,” Ph.D. dissertation, University of Minnesota, 2014.
 - [29] Q. Shi, M. Razaviyayn, Z.-Q. Luo, and C. He, “An iteratively weighted MMSE approach to distributed sum-utility maximization for a MIMO interfering broadcast channel,” *IEEE Trans. Signal Processing*, vol. 59, no. 9, pp. 4331–4340, Sept. 2011.
 - [30] L. Zhang, G. Wang, and G. B. Giannakis, “Real-time power system state estimation and forecasting via deep unrolled neural networks,” *IEEE Transactions on Signal Processing*, vol. 67, no. 15, pp. 4069–4077, 2019.
 - [31] Y. Li, M. Tofighi, J. Geng, V. Monga, and Y. C. Eldar, “Efficient and interpretable deep blind image deblurring via algorithm unrolling,” *IEEE Transactions on Computational Imaging*, vol. 6, pp. 666–681, 2020.
 - [32] Q. Hu, Y. Cai, Q. Shi, K. Xu, G. Yu, and Z. Ding, “Iterative algorithm induced deep-unfolding neural networks: Precoding design for multiuser mimo systems,” *IEEE Transactions on Wireless Communications*, pp. 1–1, 2020.
 - [33] M. Grant and S. Boyd, “CVX: Matlab software for disciplined convex programming, version 2.1,” <http://cvxr.com/cvx>, Mar. 2014.
 - [34] R. G. Bland, D. Goldfarb, and M. J. Todd, “The ellipsoid method: A survey,” *Oper. Res.*, vol. 29, no. 6, pp. 1039–1091, 1981.
 - [35] A. Liu, V. K. N. Lau, and M. Zhao, “Stochastic successive convex optimization for two-timescale hybrid precoding in massive mimo,” *IEEE Journal of Selected Topics in Signal Processing*, vol. 12, no. 3, pp. 432–444, June 2018.
 - [36] C. Peel, B. Hochwald, and A. Swindlehurst, “A vector-perturbation technique for near-capacity multiantenna multiuser communication-part I: channel inversion and regularization,” *IEEE Trans. Commun.*, vol. 53, no. 1, pp. 195–202, Jan. 2005.
 - [37] A. Shapiro, D. Dentcheva, and A. Ruszczyński, *Lectures on Stochastic Programming: Modeling and Theory*, ser. MPS-SIAM Series on Optimization. SIAM-Society for Industrial and Applied Mathematics, September 2009.
 - [38] W. Yu and R. Lui, “Dual methods for nonconvex spectrum optimization of multicarrier systems,” *IEEE Trans. Commun.*, vol. 54, no. 7, pp. 1310–1322, July 2006.
 - [39] A. Ruszczyński, “Feasible direction methods for stochastic programming problems,” *Math. Programm.*, vol. 19, no. 1, pp. 220–229, Dec. 1980.